ARTICLE

TETHYSHADROS INSULARIS, A NEW HADROSAUROID DINOSAUR (ORNITHISCHIA) FROM THE UPPER CRETACEOUS OF ITALY

FABIO M. DALLA VECCHIA

Institut Català de Paleontologia, Universitat Autònoma de Barcelona, E-08193 Cerdanyola del Vallès, Spain;
fabio.dallavecchia@icp.cat

ABSTRACT—An articulated skeleton of a hadrosauroid dinosaur, *Tethyshadros insularis* n. gen., n. sp., was recovered from the Liburnian Formation (uppermost Cretaceous) of Villaggio del Pescatore in the Trieste Province of northeastern Italy. One of the most complete dinosaur fossil ever found, it shows for the first time the entire morphology of a hadrosauroid phylogenetically close to, but outside the North American and Asiatic hadrosaurids. It lived on an island developed on a carbonate platform in the Tethys Ocean and the small size of the specimens suggests that it may be an insular dwarf. The skeleton has many peculiarities including cursorial adaptations, and a mix of derived and primitive features. European hadrosauroids probably did not evolve by vicariance nor did they colonize the European Archipelago from North America, but rather came from Asia by island hopping.

INTRODUCTION

Iguanodontoids are among the best known dinosaurs thanks to the discovery of complete and articulated skeletons of *Iguanodon* from the Lower Cretaceous of Europe and numerous hadrosaurids from the Campanian and Maastrichtian of North America. Several basal hadrosauroids phylogenetically intermediate between *Iguanodon* and hadrosaurids are reported from the Cretaceous of Asia, North America and Europe, but, excluding the basal *Dollodon,* they are represented by partial or disarticulated skeletons (Norman, 2004; Horner et al., 2004).

The first complete and articulated specimen of a primitive hadrosauroid dinosaur close to hadrosaurids is here reported from the latest Cretaceous of Italy (Fig. 1). The specimen is the most complete skeleton among medium to large-sized dinosaurs found in Europe since the 1878 discovery of *Iguanodon* and *Dollodon* at Bernissart, Belgium. It represents a new genus and species, which is described below, and its phylogenetic position, functional morphology and paleobiogeography are also discussed.

Institutional Abbreviations—FGGUB, Facultatea de Geologie şi Geofizica, Universitatea Bucureşti, Bucharest, Romania; **MCSNT**, Museo Civico di Storia Naturale, Trieste, Italy; **NHM**, The Natural History Museum, London; **SC**, Italian State collections.

SYSTEMATIC PALEONTOLOGY

ORNITHOPODA Marsh, 1882
IGUANODONTIA Sereno, 1986
IGUANODONTOIDEA Sereno, 1986
HADROSAUROIDEA Sereno, 1986
TETHYSHADROS INSULARIS, gen. et sp. nov.
(Figs. 1–8)

Etymology—*Tethys*, an ocean that occupied the general position of the Alpine-Himalayan orogenic belt, and *hadros* for hadrosauroid, "Tethyan hadrosauroid"; *insularis* after the Latin *insular* for island dweller.

Holotype—SC 57021, complete and articulated skeleton (Fig. 1).

Referred Material—SC 57022, partial, articulated forelimbs, possibly from a complete skeleton still in situ; SC 57023, an isolated left pubis; SC 57025, an isolated cervical vertebra with the right rib; SC 57026, a complete, but strongly crushed, skull and most of the lower jaws, with some parts of the postcranium, from an apparently complete skeleton affected by subaqueous sediment slumping; SC 57247, part of an articulated and probably complete skeleton that was damaged during extraction; SC 57256, an isolated dorsal rib. All the specimens are at the MCSNT.

Horizon and Locality—A lens of well-bedded, black limestone, 10 meters-thick and 70 meters long, in the upper Campanian–Paleocene Liburnian Formation near the Villaggio del Pescatore, Trieste Province, north-eastern Italy. The whole lens possibly formed in less than 10,000 years (Arbulla et al., 2006). SC 57021, SC 57023, SC 57025, SC 57026, SC 57247, and SC 57256 come from different levels within the lens. The occurrence of the foraminifer *Murciella cuvillieri* immediately below the bone-bearing lens (Dalla Vecchia, 2008), its range (Steuber et al., 2005), and the stratigraphic framework of the Karst Plateau (Jurkovšek et al., 1996; Venturini et al., 2008), suggest a late Campanian–early Maastrichtian age for *Tethyshadros*. The presence of the alligatoroid *Acynodon* (Delfino and Buffetaut, 2006) further supports this age (Martin, 2007).

Diagnosis—Hadrosauroid dinosaur with the following autapomorphies: skull large (skull length 1.60–1.65 times humeral length) and elongate (skull length:height ratio ∼2.6); premaxillary denticles very large, slender and pointed; small paired crests in caudal part of parietals; jugal very long, slender, without ventral flange, portion caudal to dorsal process more than twice length of rostral process; infratemporal fenestra subrectangular and large, nearly twice orbit size; lateral distal condyle of quadrate flared and ventrally flat (nail-head shaped); first caudal centra longer than high; neural spines of proximal caudal vertebrae 1-6, and possibly also distal dorsals and sacrals, hatchet-shaped; ribs of caudal vertebrae 1–5 tongue-shaped, craniocaudally wide and dorsoventrally flattened; long, whip-like mid- to distal part of tail with elongated vertebral centra, 2.4 to 3.4 times longer than high at mid-centrum in caudal vertebrae 18 to 32; centra of caudal vertebrae 23 to 33 with shape of semicylinders; a long segment of proximal caudal vertebrae without haemapophyses (first chevron between caudal vertebrae 7 and 8) and consequently, there is a ventral "gap" representing 44% of the preserved holotype tail segment; distal end of haemapophyses
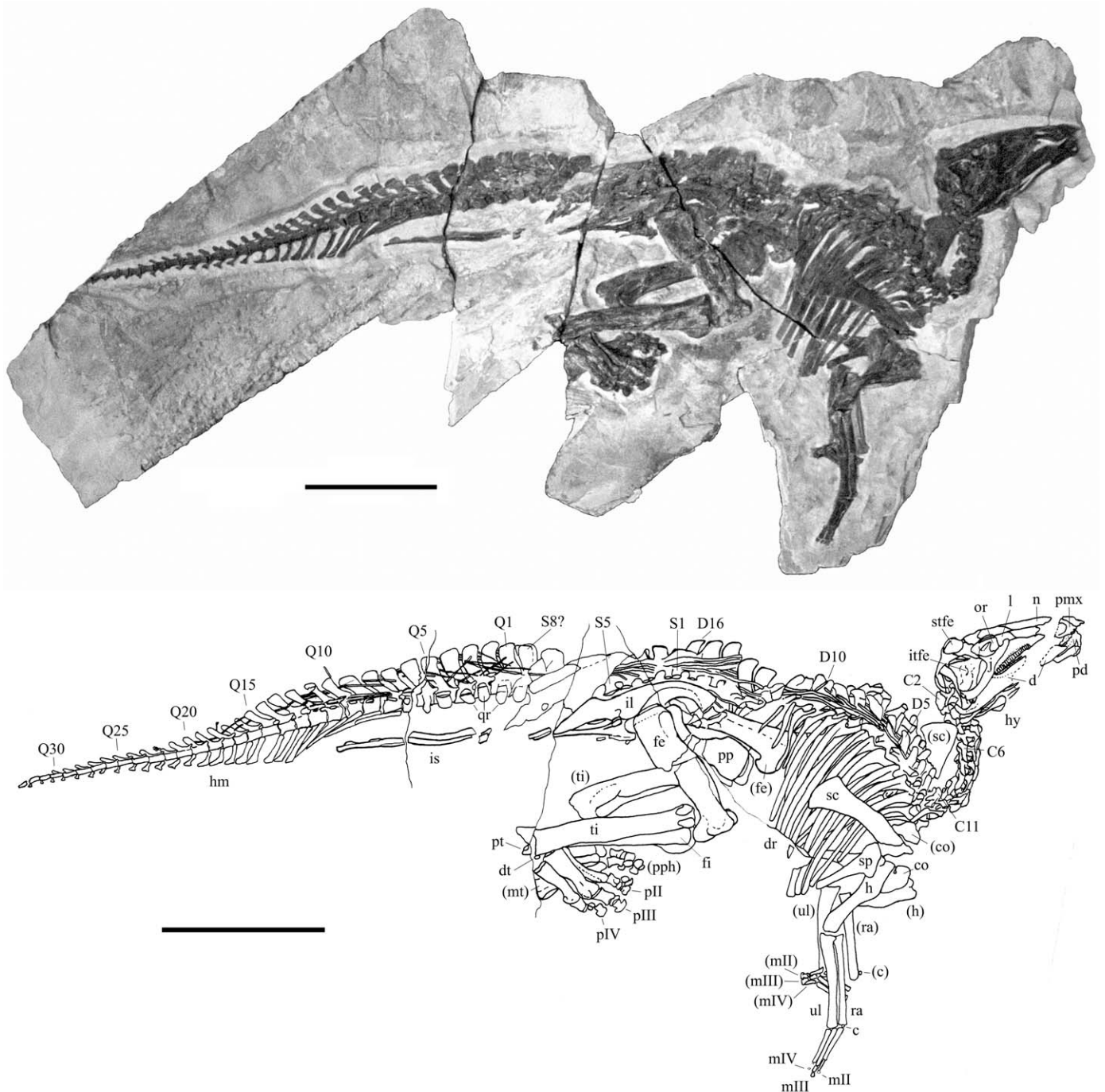
FIGURE 1. Skeletal anatomy of *Tethyshadros insularis*, SC 57021, holotype. **Abbreviations**: **C**, cervical vertebra; **c**, carpal; **co**, coracoid; **D**, dorsal vertebra; **d**, dentary; **dr**, dorsal rib; **dt**, distal tarsal; **fe**, femur; **fi**, fibula; **h**, humerus; **hm**, haemapophyses; **hy**, first ceratobranchial (hyoid apparatus); **j**, jugal; **il**, ilium; **is**, ischium; **itfe**, infratemporal fenestra; **l**, lacrimal; **mII–IV**, manual digits II–IV; **mt**, metatarsus; **n**, nasal; **or**, orbit; **pII–IV**, pedal digits II–IV; **pd**, predentary; **pmx**, premaxilla; **pp**, prepubic process of pubis; **pph**, pedal phalanges; **pt**, proximal tarsals; **Q**, caudal vertebra; **qr**, caudal rib; **ra**, radius; **S**, sacral vertebra; **sc**, scapula; **sp**, sternal plate; **stfe**, supratemporal fenestra; **ti**, tibia; **ul**, ulna. Left-side elements are in parentheses. Scale bar equals 500 mm.

in vertebrae 15–20 with a long posterior process; scapular blade asymmetrically expanded distally (like the primitive iguanodontians *Camptosaurus* and *Dryosaurus*); postacetabular process of ilium long, low, blade-like (no brevis shelf), triangular and tapering in lateral view; very long ischium with a sigmoid shaft and blunt, unexpanded distal end, not bent nor tapering; only three manual digits (digit V lost); flat distal articular end of metacarpals; only two phalanges in manual digit IV, distal one very reduced (lost phalanx 2 of other hadrosauroids); tibia considerably longer than femur. It also has the following unique combination of characters: low ilium with large and pendant supracetabular process and robust preacetabular process not markedly arched and without dorsal depression at the supracetabular process.

TERMINOLOGY AND METHODS

The Hadrosauridae are considered as the Hadrosaurinae, the Lambeosaurinae and all descendents of their most recent common ancestor, following Prieto-Marquez et al. (2006). Hadrosauroids are all dinosaurs more closely related to *Parasaurolophus* than *Iguanodon*, following Sereno (1998).

In the description, I used the anatomical terminology of Norman (2002), Horner et al. (2004) and Evans and Reisz (2007). Zygapophyses, parapophysis and diapophysis are considered in their original meaning of processes, not as synonymous of zygapophyseal, parapophyseal and diapophyseal facets. The proximal caudal vertebrae are those with a distinct fused rib, the middle caudal vertebrae are those without a rib, but bearing a chevron, whereas the distal caudal vertebrae lack a chevron.

I based the comparison with *Telmatosaurus* on Weishampel et al. (1993) and on the direct observation of the material attributed to this taxon deposited at NHM. In addition to the actual specimen, a cast (deposited at MCSNT) made when the forelimbs of SC 57021 were exposed on the side opposite to that visible in the mounted specimen, was used in the description of the holotype. The length of the skull is measured from the tip of the premaxillary denticles to the caudal end of the paroccipital process; its height is measured between the distal condylar surface of the quadrate and the dorsal surface of the squamosal. The length of the humerus is measured as the straight line between the distal and proximal extreme points. The orientation of the skeletal elements is that observed in mounted skeletons of hadrosauroids and in the articulated holotype. The hand is described with the palmar surface oriented medially and touching the ground in a quadrupedal (resting) stance; consequently the surface opposite to the palmar is the lateral one and the outer margin of metacarpal II faces cranially.

DESCRIPTION

All the specimens were originally preserved in limestone beds. Only SC 57025 and the predentary and the premaxillae of the holotype were completely freed from the rock by chemical methods. SC 57247 is still unprepared. Two syndepositional faults formed prior to lithification crossed the holotype skeleton at the caudal end of the torso and at the base of the tail; SC 57022 and SC 57026 are also affected by syndepositional faults. The tail is incomplete distally because the tip was not excavated and remained in the site. A dissolution fissure crosses the skull, and some phalanges of the right hand are strongly weathered. Otherwise, the skeleton is complete. It is 3620 cm long measured from the tip of the snout to the distal end of the tail, which is small for a hadrosauroid (Weishampel et al., 1993; Norman, 2004; Horner et al., 2004). SC 57247 and SC 57022 represent individuals larger and possibly more robust than the holotype, whereas SC 57026 is approximately similar in size, and SC 57023 is a smaller individual. Fusion of vertebral centra and neural arches, the presence of barely visible sutures between many skull elements, the degree of ossification, the skull elongation and the relative size of the orbit do not support a juvenile status for the holotype (Carpenter, 1994; Horner and Currie, 1994). When not otherwise specified, the description is based on the holotype specimen.

Skull

The skull (Fig. 2) is 475 mm long and about 185 mm tall (the caudal part of the skull is slightly deformed by crushing); length/height ratio is 2.57. It is more elongated than the skull of most hadrosaurids (only *Edmontosaurus annectens* may have a more elongated skull, ratio up to 3.4; Horner et al., 2004). Among basal hadrosauroids it is matched by *Dollodon bampingi* and exceeded only by *Ouranosaurus nigeriensis* (ratios 2.6 and 3.2 respectively; Norman, 2004; Horner et al., 2004; Paul, 2008). As

for the overall outline, it resembles the basal-most hadrosauroids *D. bampingi* and *Mantellisaurus atherfieldensis*. In the postorbital region and dorsal view, the cranium is relatively broad transversely, as in *Iguanodon*, and lacks the distinctive caudal narrowing observed in most hadrosaurids and *Ouranosaurus*.

Fenestrae—The external naris is relatively short (no longer than 75 mm and probably slightly less). Its caudal terminal portion is narrow, slit-like with a rounded end; there is no trace of a caudal extension of the circumnarial fossa. It is small relative to skull length as in basal hadrosauroids (Paul, 2008), external naris length:skull length ratio being about 0.15. In contrast, it is 0.35 in the hadrosaurids *Gryposaurus notabilis* and *Prosaurolophus maximus*, and 0.32 in *Edmontosaurus regalis*, based on figures in Lull and Wright (1942). The orbit is dorsocaudally to ventrorostrally elongated, with a maximum axial length of 85 mm and a perpendicular length of 55 mm. The infratemporal fenestra is very large, and dorsocaudally to ventrorostrally elongated. Deformation of the caudal part of the skull due to crushing and the ventral shifting of the jugal has slightly modified the original subrectangular shape of the fenestra (Fig. 2B). The maximum axial length is 120 mm (dorsocaudal–ventrorostral) and the perpendicular height is 104 mm; it is about two times wider than orbit. The supratemporal fenestra is oval, mediocaudally to rostrolaterally elongated, relatively short, with a maximum axial length of 63 mm and a perpendicular width of 45 mm. It is exposed dorsolaterally because of crushing. An antorbital opening is absent, but an elliptical depression occurs at the top of the dorsal process of the maxilla, just rostral to the jugal and ventral to the lacrimal.

Premaxilla—The premaxillae are not completely fused each other and the left one is slightly displaced rostrally. Although they are crushed lateromedially reducing their width, it is evident that the muzzle was not much expanded laterally. The premaxillary rostral margin in dorsoventral view was probably U-shaped, not broadly arcuate as in the Hadrosaurinae. The oral margin is coarsely denticulate, with the symphyseal denticle the largest, the second slightly smaller and the third much reduced. They are spike-like and directed forward. The first two are long and slender resembling the predentary denticles of *Iguanodon* (see Norman, 1980). Large foramina occur immediately dorsodistally from the two larger denticles. The caudal part of the narial fossa was destroyed; the preserved rostral part does not reach the rostral termination of the external naris. There is no accessory narial fossa. Small foramina pierce the rostrolateral surface of the narial fossa and the ventral surface of premaxilla. The largest occurs close to the rostral edge of the fossa, but it is much smaller than the premaxillary foramen of hadrosaurids and cannot be positively identified as such. The caudodorsal process seems to end level with the caudal end of the external naris, although this is difficult to confirm because the suture with the nasal is nearly completely obliterated. The caudolateral process forms the ventral edge of the caudal part of the external nares; the caudal termination of the process tapers between the prefrontal and the lacrimal.

Maxilla—The maxilla is triangular in lateral view, 180 mm long and 58 mm high (including the teeth), with the triangular dorsal process at the midpoint. A thin alveolar parapet covers the tooth battery buccally. A longitudinal ridge, slightly arched and rounded, represents the dorsal margin of the cheek recess. Unlike hadrosaurids, there is no evidence of a large maxillary foramen in the rostrodorsal part of the maxilla. Three foramina are visible roughly aligned along the middle of the lateral wall of the maxilla; two are close to each other and located ventral to the jugal articulation, the other is placed much rostrally. The rostroventral end of the jugal rests on a low, laterodorsal process of the maxilla as in *Telmatosaurus* and the Hadrosauridae, not on a finger-like process as in *Iguanodon* and some basal hadrosauroids such as *Mantellisaurus* and *Ouranosaurus*.
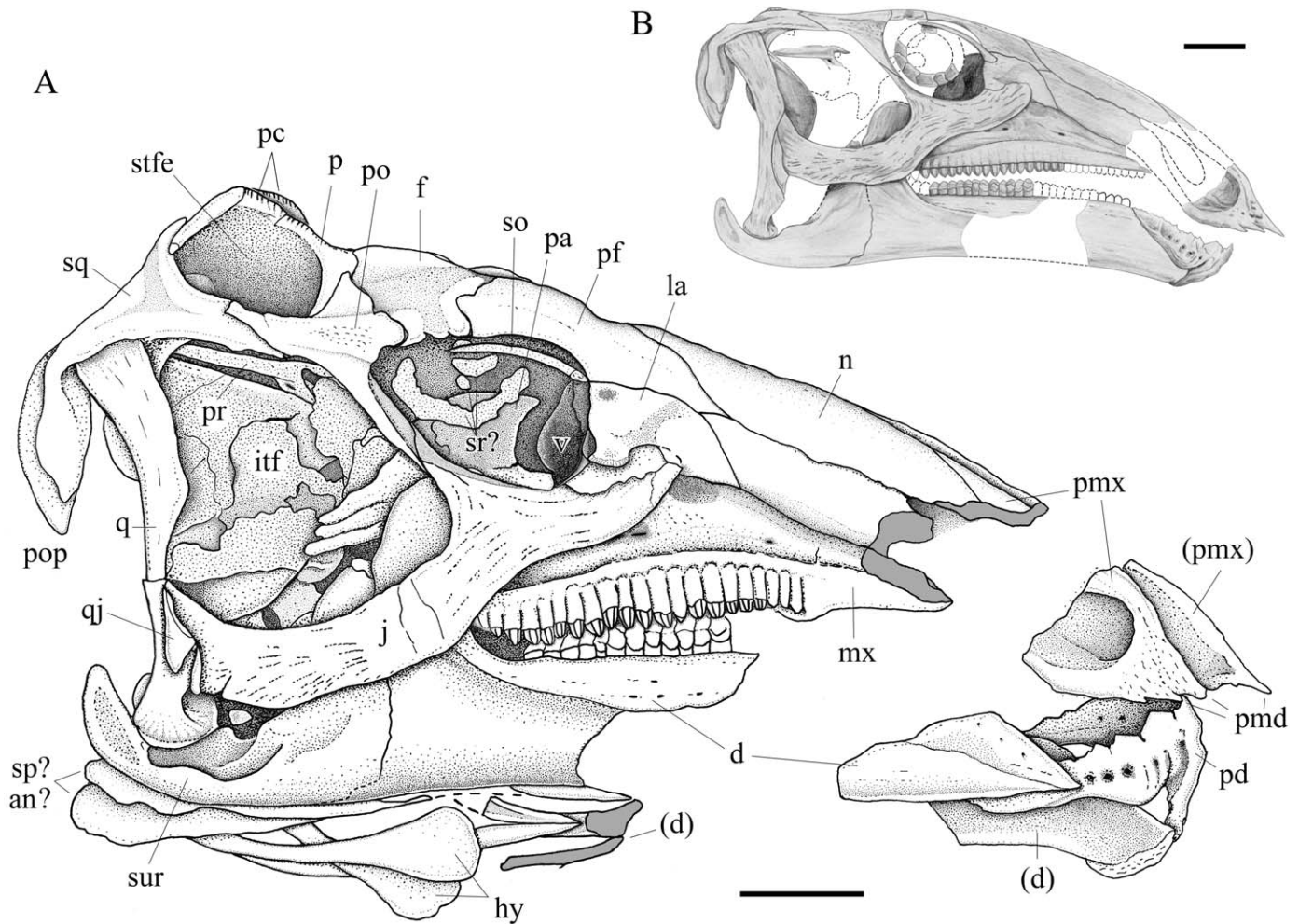
FIGURE 2. Skull and the lower jaw of *Tethyshadros insularis*, SC 57021, holotype. **A**, the bones as preserved; **B**, reconstruction. **Abbreviations**: **an**, angular; **d**, dentary; **f**, frontal; **hy**, first ceratobranchial (hyoid apparatus); **j**, jugal; **itf**, infratemporal fenestra; **la**, lacrimal; **mx**, maxilla; **n**, nasal; **p**, parietal; **pa**, palatine; **pc**, paired parietal crests; **pd**, predentary; **pf**, prefrontal; **pmd**, premaxillary denticles; **pmx**, premaxilla; **po**, postorbital; **pop**, paroccipital process; **pr**, prootic; **q**, quadrate; **qj**, quadratojugal; **so**, supraorbital; **sp**, splenial; **sq**, squamosal; **sr**, sclerotic ring bones; **stfe**, supratemporal fenestra; **sur**, surangular; **v**, vomer. Left-side elements are in parentheses. Shaded areas in outline represent regions where the bone is cross-sectioned. Scale bar equals 50 mm.

Nasal—The nasal in laterodorsal view is a long, slender bone with pointed extremities. Its dorsal margin is only slightly curved, giving the rostrum a gently convex outline. The suture with the caudodorsal process of the premaxilla in lateral view extends diagonally above the posterior part of the external naris. The suture with the caudolateral process of the premaxilla seems to start at the posterior apex of the external naris and extends straight to the rostral point of the prefrontal, then diagonally towards the midline as the nasal-prefrontal suture. The nasal forms the dorsal edge of the caudal part of the external nares.

Lacrimal—The lacrimal is subtrapezoidal in lateral view. It is sutured dorsally with the prefrontal, rostrally with the caudolateral process of the premaxilla, ventrorostrally with the dorsal process of the maxilla and ventrocaudally with the rostral process of the jugal. The lacrimal forms the rostral border of the orbit. It has a rostral acute point like the lacrimal of *Equijubus*, *Telmatosaurus* and hadrosaurids (Nopcsa, 1900; You et al., 2003; Horner et al., 2004). A ventral process extends to a dorsal, notched facet on the jugal. The ventral end of the process is slightly expanded and thickened. The corresponding facet of the

jugal has a thickened rim. The mid–ventral marginal part of the lacrimal is overlapped by the rostral process of the jugal. The ventral margin is higher than the apex of the dorsal process of the maxilla on the lateral side of the skull as in *Equijubus*, *Telmatosaurus*, and hadrosaurids, but unlike *Iguanodon*, *Dollodon* and *Ouranosaurus*. The caudal (orbital) side is lateromedially narrow and deeply concave (grooved) for the lacrimal foramen. The lateral surface shows a small pit at the dorsocaudal corner, just below the suture with the prefrontal, probably for the articulation of the supraorbital.

Prefrontal—The prefrontal is a rather large and craniocaudally elongated element (120 mm long), twice as large as the lacrimal, and slightly convex dorsally. It forms the rostral half of the upper orbital margin and extends rostrally as a wedge tightly sutured between the lacrimal and the nasal. The distal point contacts ventrally the dorsal margin of the caudal termination of the caudolateral process of the premaxilla. All the sutures with those bones are barely visible. Caudally and caudomedially, it is loosely sutured to the frontal. It sends a small process into the rostral margin of the frontal.

Frontal—The frontal is wide and flat, with a rostral and a lateral flange. The rostral flange contacts the nasals rostrally and the prefrontal laterally; it is difficult to ascertain its actual shape because of crushing. However, it is rather narrow and long, and its rostral termination may be tapered. The rectangular lateral flange forms part of the dorsal margin of the orbit; it bears three terminal 'denticles' with a rough lateral and ventral surface. The sigmoid, caudolateral suture with the postorbital is open like that with the prefrontal, whereas the caudomedial straight suture with the parietal is barely distinguishable.

Parietal—The parietals are fused along the midline forming a flat sagittal surface separating the supratemporal fenestrae. This surface is narrow and expanded at both ends. The segment between the two expanded extremities is short, less than half the length of the supratemporal fenestra. A pair of small, but well-formed crests with striated and rough dorsal margins project from the lateral edge of the sagittal surface along the caudomedial margin of each fenestra (Fig. 2A). The parietal sends a lateral process, which forms the whole rostral margin of the supratemporal fenestra, and is sutured rostrally to the caudal side of the medial process of the postorbital. The parietal is probably overlapped caudolaterally by the medial process of the squamosal.

Postorbital—The body of the tetraradiate postorbital is inflated, thickened and with a rough surface. The rostral process is small, triangular and sutured to the frontal. A notch separates it rostromedially from the wide, wing-shaped medial process that is sutured rostrally to the frontal, medially and caudally to the parietal. The long caudal process overlaps the cranial process of the squamosal and forms slightly more than half the lateral margin of the supratemporal fenestra and less than half the dorsal margin of the infratemporal fenestra. The ventral process is also long and bar-like, flattened caudorostrally and with a slightly concave rostral surface that forms the caudal margin of the orbit. It is directed ventrorostrally and meets the dorsal process of the jugal.

Squamosal—The squamosal forms the posterodorsal corner of the skull. It bears a large and deep cotylus, which is bordered by two descending processes, for the proximal head of the quadrate. The prequadratic process borders rostromedially the cotylus and is shorter than quadrate condylus breadth. The large, lateromedially flat, postquadratic process is leaf-shaped and forms the rostrolateral part of the paroccipital process. A large, rostrocaudally long and dorsoventrally flat rostral process is overlapped dorsocranially by the caudal process of the postorbital. It forms more than half the upper margin of the infratemporal fenestra and less than half the lateral margin of the supratemporal fenestra. The medial process forms the caudal edge of the supratemporal fenestra and is broken in the middle because of crushing.

Supraorbital—A thin, rod-like supraorbital bone is preserved inside the orbit, just below its dorsal margin. It has a curved shaft that is slightly expanded rostrally and slightly tapering caudally. As exposed, it has the same curvature as the dorsal edge of the orbit. The surface at the caudal end is rough. The supraorbital occurs in many basal hadrosauroids and more primitive iguanodontians like *Camptosaurus* and *Iguanodon*, where it articulates laterally on the lacrimal or prefrontal (Norman, 2004); it is fused to the prefrontal and postorbital in hadrosaurids (Maryańska and Osmólska, 1979). Although the rostral end contacts the rostral rim of the orbit at the prefrontal–lacrimal suture in SC 57021, comparison with other iguanodontians suggests that originally it articulated in a small pit on the dorsocaudal corner of the lateral side of the lacrimal.

Jugal—The jugal is the longest cranial bone, excluding the premaxilla, being 195 mm long from the extremity of the rostral process to that of the caudal process. It is elongated and robust, but also slender. It is narrow dorsoventrally and uniform in height along its entire length. As seen in lateral view, it contacts the lacrimal along the dorsal margin of the rostral process, the maxilla along its lower margin, and the quadratojugal, and possibly the quadrate as well, with the end of the caudal process. The ventral edge of the caudal process is gently convex; it is concave below the dorsal process and again becomes slightly convex in the rostral process. The rostral termination is unexpanded, with a leaf-like outline and a smoothly rounded margin. It is more similar to that of *Bactrosaurus* (see Godefroit et al., 1998), *Tanius* (see Wiman, 1929) and possibly *Gilmoreosaurus* (see Gilmore, 1933) than to the dorsoventrally expanded, angular and pointed rostral termination of *Telmatosaurus* and most Hadrosaurinae, and to the tapering and pointed rostral process of *Iguanodon*, *Mantellisaurus* and *Dollodon*. It is dorsally notched for the caudoventral process of the lacrimal. The triangular dorsal process tapers to a rostrocaudally flattened bar that meets the ventral process of the postorbital at mid-orbit. The caudal process is very long, strap-like and has a gently concave dorsal edge that forms the lower margin of the wide infratemporal fenestra. There is no ventral flange behind the level of the dorsal process as is the case of many hadrosaurids (Horner et al., 2004). The caudal end of the caudal process is blade-like and curves dorsally without flaring.

Quadrate—The quadrate has a vertical shaft (caudal ramus), with the dorsal half bent caudally. The caudodorsal 'squamosal' protuberance (Prieto-Marquez et al., 2006, suppl. data) is absent. The cranial edge of the lateral wing has a long and relatively shallow embayment for the quadratojugal, and possibly for the dorsal end of the caudal process of the jugal. The embayment is symmetrical and not centered on the middle-third of the quadrate, but is displaced ventrally. The external mandibular condyle is large and flared, with a nearly flat articular surface, and resembles a nail-head in lateral view (Fig. 2A). A flat articular surface is also seen in SC 57026. The medial condyle of SC 57026 is only slightly smaller than the lateral condyle, and has an oval and slightly concave articular surface. The two condyles are separated by a wide, shallow groove. As in *Iguanodon*, they are of the same height. The external mandibular condyle of the hadrosauroids is usually hemispheric or at least convex, and not flared (Nopcsa, 1900; Gilmore, 1933; Norman, 1986, 2002; Godefroit et al., 1998; Horner et al., 2004). In the hadrosaurids, the medial condyle is much smaller than the lateral condyle and placed higher (Horner et al., 2004).

Quadratojugal—The quadratojugal has shifted ventrally from its original location inside the embayment of the quadrate. It is bent and broken against the ventral part of the lateral wing of the quadrate, wrapping around it. It is a laterally flat bone, with thicker caudal and caudoventral margins. Its outline is not clear, but the shape of the quadrate embayment and size and shape of the caudal end of the jugal, suggest that it was dorsoventrally elongated and rostrocaudally very narrow. Probably it did not occupy the whole embayment. The upper part of the embayment was consequently contacted by the jugal.

Palate—The dorsal part of the plate-like palatine is exposed inside the orbit. It is lateromedially flattened, with a deeply concave rostral margin giving it an arched aspect. It occurs in a more caudal position as compared to *Iguanodon* (see Norman, 1980) and *Edmontosaurus* (see Lambe, 1920). The caudal end of the dorsal plate of the vomer is visible rostral to the palatine. Although a pterygoid cannot be distinguished because of crushing, probably its wide and thin quadrate ramus participates, with the broad pterygoid wing of the quadrate, to the sheet of bone extending along the inner wall of the infratemporal fenestra.

Braincase—The exoccipital forms the caudal portion of the pendent, distal part of the paroccipital process, which is straight, leaf-shaped and ventrally directed. The prootic is a caudorostrally elongate, dorsoventrally narrow and rostrally "bifurcated" bone, occurring parallel to the squamosal–postorbital bar beneath the parietal (Fig. 2A). It resembles the prootic of *Tanius*

sinensis (see Wiman, 1929:pl. V, figs. 6-7). The large cranial foramen is that of the trigeminal nerve (CN V); the smaller, elongate and narrow foramen that pierces the ventral ramus of the "fork" could be the foramen for the facialis nerve (CN VII).

Sclerotic Bones—Remnants of extremely thin, flat and smooth bones inside the orbit are tentatively identified as the elements of a sclerotic ring. Sclerotic bones occurs in hadrosaurids (Horner et al., 2004), but they are not reported in basal hadrosauroids (Norman, 2004).

Lower Jaw

The lower jaw is slender and long, with the two rami unfused at the symphysis.

Predentary—The predentary, compressed lateromedially and deformed, has an U-like profile in plan view, with sigmoid lateral processes. It is at least 85 mm long and 39 mm wide, but width is reduced by crushing; height is 62 mm including the median (ventral) process. The latter is very large, robust and strongly bifurcated, and projects from the middle of the rostroventral edge of the transverse ramus. It is followed caudally by a knob-like, median dorsal process. The oral margin bears labiolingually flattened denticles decreasing in size caudally and morphologically unlike the premaxillary denticles. The symphyseal ones are the largest and have a subpentagonal outline because of deep basal notches separating them each other and from the adjacent denticles. At least two, roughly triangular denticles decreasing in size follow distally in the right and better preserved lateral process. A much smaller accessory denticle arises between those denticles and distal to the distal one. Probably denticles covered most of the dorsal margin of the process, but are damaged. A prominent vascular groove occurs on each side of the midline of the transverse ramus in a manner similar to *Probactrosaurus* (see Norman 2002, fig. 10C). Grooves extend ventrally from a pair of large foramina located at mid-height. The lateral processes are relatively low and taper caudally; the dentary (ventral) side is flat and thick in ventral view and straight in lateral view. The external side of each lateral process is pierced by a row of at least five large foramina, which are located in pits, that open to the medial side. The caudal end of the process is slightly expanded lateromedially and ventrally flat, fitting in a notch on the dentary.

Dentary—The distal end of the dentary is bent mediorostrally in a short symphysis bearing a narrow and rough symphyseal surface; it does not seem to be deflected ventrally. A row of neurovascular foramina occurs laterally, close to the surface of articulation with the predentary. This narrow, long, and sloping surface has a median longitudinal groove and ends caudally with a shallow notch that received the caudal end of the predentary. The dentition begins just caudal to this notch. The middle portion of the dentary is not preserved. A wide shelf occurs dorsally along the middle to caudal part of the dentary up to the base of the coronoid process, and is pierced by several foramina; its continuation medial to the coronoid process cannot be verified. The dentary forms the rostral and apical part of the coronoid process. This process is curved rostrally, with the apex somewhat expanded, but not completely visible or preserved in either specimens. The suture between the dentary and the surangular crosses vertically the wide base of the coronoid process as a median and straight line, and seems to turn caudally only near the ventral margin of the lower jaw. The caudoventral end of the dentary is slightly caudal to the apex of the coronoid process.

Surangular—The surangular is a large bone forming most of the caudal part of the mandibular ramus and conspicuously contributing to the caudal part of the coronoid process. Caudal to the adductor fossa, the bone broadens lateromedially; here a cup-shaped, wide and shallow glenoid occurs that is divided into a rostral (larger) and a caudal depression separated by a low, transversal ridge. The lateral condyle of the quadrate is articulated in the caudal depression, which is probably in the articular, although no suture is visible. The lateral margin of the glenoid is bordered by a thick, wing-like lip projecting laterodorsally. There is no surangular foramen along the lateral surface. The upturned retroarticular process is long and robust, and angled 115° with the axis of the mandible.

Angular and Splenial—The angular cannot be readily identified ventral to the surangular. Two elongated and paired bones along the caudoventral edge of the right lower jaw ramus are tentatively identified as detached splenials (although their position would be more caudal than in other hadrosauroids; e.g., Norman, 1986) or angulars. Their caudal portion is flattened and expanded.

First Ceratobranchials—Two paired first ceratobranchials of the hyoid apparatus are preserved in their anatomical position just ventral the caudal part of the mandible. They have a very slender, rod-like, curved shaft, and a rostral extremity broadly expanded, flat and spatula-shape. The edge of the expanded extremity is slightly thickened and rounded.

Dentition

Maxillary Teeth—Maxillary teeth are in situ on the right maxilla of the holotype and on the right maxilla of SC 57026. They are scattered in the region of the broken and crushed left maxilla of SC 57026. Twenty-one tooth families can be counted in the right maxilla of the holotype, but the rostral part of the bone is damaged and single families cannot be recognized. Considering the length of the damaged part (50 mm) and the mesiodistal width of the functional crowns (about 5 mm), an additional 10 tooth families may have been present. Thus, the count of the tooth families exposed in lateral view would have been 31. Because of tooth size and the vertical space available to accommodate the replacement teeth in each tooth row, it seems rather unlikely that there are more than two replacement teeth at any one time. The tooth crown is elongate, symmetrical and narrow, with roughly parallel mesial and distal margins that converge apically into a rounded apex in unworn teeth. The apicobasal height of the most complete tooth in SC 57026 is 23 mm (possibly a small portion of the base is covered, thus the crown could be slightly higher); the maximum mesiodistal width is about 6 mm. The main feature is a robust median carina, buccally projecting and strongly arcuate, which occupies most of the buccal side of the crown, leaving distally and mesially only very narrow, flat marginal areas. A thin, secondary basoapical ridge crosses the mesial marginal area and the basal part of the median carina of some teeth. The mesial margin has lingulate denticles, each prolonged for a short distance as a thin ridge into the marginal area of the crown. The distal margin, always poorly preserved, has denticles too.

Dentary Teeth—The rostral segment of the left dentary preserves remains of four closely packed teeth belonging to the first three tooth families (the first tooth family shows two teeth). Dentition begins immediately caudal to the surface for the articulation of the predentary, thus there is no diastema. The crowns are lanceolate. The crown of the erupting replacement tooth of the third family, the most complete, is at least 15 mm high, a maximum of 5 mm mesiodistally wide, and slightly asymmetric. The distal edge of the upper part of this crown has denticles that continue onto the lingual surface with short, wide and blunt ridges; small, pointed denticles occur along the upper mesial margin. Only a robust and straight median carina and no subsidiary ridges, is observed on all three crowns. More distal mandibular teeth are visible only in occlusal view in the holotype, but 15 consecutive dentary families of the middle to proximal dentary teeth can be observed in lingual view in the right dentary of SC 57026 (Fig. 3). There are two functional teeth per tooth
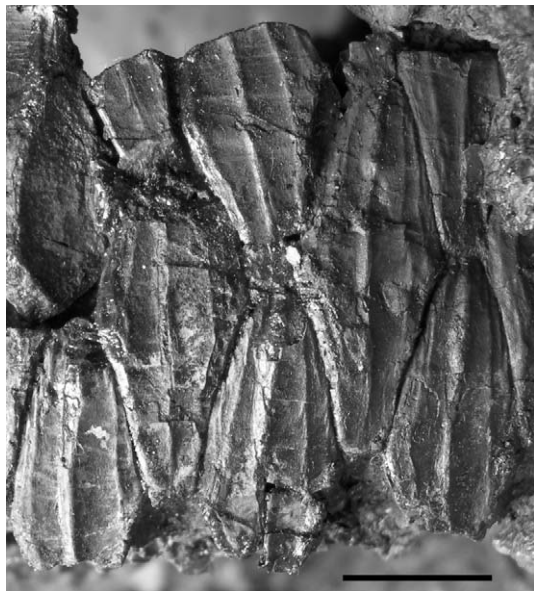
FIGURE 3. Right dentary teeth of *Tethyshadros insularis*, SC 57026, lingual view. Scale bar equals 10 mm.

position, and their shear surfaces are oriented buccally. The exact number of replacement teeth per tooth family cannot be observed directly, but the presence of more than two replacement teeth is improbable because of the height of the dentary. The teeth are closely packed to form a dental battery. The crown is lanceolate, with an angled distal margin (the apex of the angle is at mid-height) and a more rounded mesial margin with maximum curvature occurring slightly below the mid-height of the crown (i.e., lower than the apex of the distal angle). This gives the crown a slightly asymmetric profile. Dentary teeth are larger than maxillary teeth. The maximum mesiodistal width of a mid-dentary replacement tooth crown is 10 mm and its apicobasal height is 25 mm. The apex is only slightly asymmetric and the upper part of the crown is not curved backward like the tooth of *Telmatosaurus* figured in Weishampel et al. (1993). Three to four marginal, lingulate denticles are well-exposed along the upper mesial margin only in the lower replacement teeth. The denticles of upper replacement teeth are probably very small and difficult to identify because the crowns are closely packed, but their presence is suggested by the ridging pattern. The thin, distinct, median carina is more prominent than the distal and mesial subsidiary ridges, which show some variation in the different teeth. The only complete replacement tooth crown (Fig. 3) has a slightly sigmoid median carina and a thin, distal subsidiary ridge parallel to it, beginning close to the apex of the crown and ending in its lower part. A second, shorter ridge occurs more distally, beginning lower on the margin. A much shorter third ridge occurs close the distal margin just dorsal the zone of maximum width of the crown. The mesial half of this crown shows two thin subsidiary ridges with the same orientation of the distal ones. The mesial margin of upper replacement teeth is poorly preserved and further details cannot be observed. The two mesial subsidiary ridges start from marginal denticles in the lower replacement tooth crowns. The outer ridge extends to the lower half of the crown parallel to its edge, whereas the inner ridge is limited to the upper half. Additional subsidiary ridges, which are faint and short, occur in the better preserved lower crowns, starting from the mesial denticles. A lower replacement crown has a single, thin, distal subsidiary ridge. A few lower replacement crowns seem to lack subsidiary ridges at all, having only a thickened rim along the mesial and distal edges.

The crown–root angle, observed in a slightly displaced tooth, is about 130°.

Axial Skeleton

The complete and articulated axial skeleton will be described in detail elsewhere. Here only essential aspects are reported. The first rib undoubtedly involved in the rib cage articulates on presacral vertebra 12, which for the count of cervical and dorsal vertebrae, I consider as the first dorsal vertebra. Therefore, the vertebral column is composed of 11 cervical vertebrae, 16 dorsal vertebrae, probably 8 sacral vertebrae (see below) and >33 caudal vertebrae.

Cervical Vertebrae and Cervico–dorsal Transition—The transition between the neck and torso occurs in the point of maximum curvature of the vertebral column. There is a gradual change in morphology from cervical to dorsal vertebrae involving pre- and postzygapophyses, diapophyses, parapophyses and neural spines.

The neural arches of atlas and axis are similar to those of *Iguanodon* (Norman, 1980). The centra of the other cervical vertebrae are opisthocoelous. The length of the visible part of the centrum ($\sim$ 40–45 mm) is roughly corresponding to the neural arch height. The prezygapophysis and diapophysis in presacral vertebrae 3 to 13 are borne by an angled 'transverse process' like in *Iguanodon* and hadrosauroids. In the dorsal vertebra 3, the prezygapophyseal facet extends on the whole dorsal side of the 'transverse process,' whereas beginning at dorsal vertebra 4, the cranially projecting prezygapophysis is separate from the true transverse process. From cervical vertebra 4 to 9, the postzygapophysis forms a caudally projecting postzygapophyseal 'peduncle,' which becomes gradually shorter in cervical vertebrae 10 and 11 and dorsal vertebrae 1 and 2. The postzygapophysis is much smaller in dorsal vertebra 3 and resembles those of the following dorsal vertebrae. The postzygapophyses are probably above the level of the neural canal but not much higher, and they are not very arched dorsally nor are dorsocaudally directed as in hadrosaurids and possibly *Telmatosaurus*. The neural spines in vertebrae 3 to 10 are very low and with a hooked apex. The neural spine of cervical vertebra 11 is larger than the preceding, and resembles that of the first dorsal vertebra.

Cervical Ribs—The ribs of cervical vertebrae 4 to 8 (and possibly 9), are similar to those of *Iguanodon* (see Norman, 1980). In the rib of cervical vertebra 10, the tuberculum is shorter and the capitulum longer than that of the preceding ribs and the shaft is rod-like and much longer, but a cranial-projecting spine is still present. The rib of the cervical vertebra 11 has the overall aspect of a dorsal rib. The tuberculum is sutured to the diapophysis in SC 57025, with a suture partly obliterated, and the capitulum is sutured as well.

Dorsal Vertebrae—Dorsal vertebra 13 is the last to bear a rib and has a transverse process like those of the preceding dorsal vertebrae. The following three vertebrae have transverse processes gradually transitional in shape to the diapophyses of the sacral vertebrae. They are included in the dorsal count (with a total of 16 vertebrae) because vertebrae in the same position are not reported as sacral vertebrae in other hadrosauroids (Parks, 1920; Prieto-Marquez, 2007), and because *Iguanodon* and hadrosauroids have 16 or more dorsal vertebrae (Norman, 2004; Horner et al., 2004). However, dorsal vertebra 16 could actually be considered a dorsosacral. The circular and concave parapophyseal facet of dorsal vertebra 2 and 3 occurs just at the base of the transverse process. The neural spine of the first dorsal vertebra resembles that of the last cervical. The spines of the following dorsal vertebrae are relatively low and craniocaudally wide. In dorsal vertebrae 12 to 16, they are possibly hatched-shaped like those of the first caudal vertebrae, but this cannot be ascertained because they are ventrally covered by the bundles of ossified tendons.
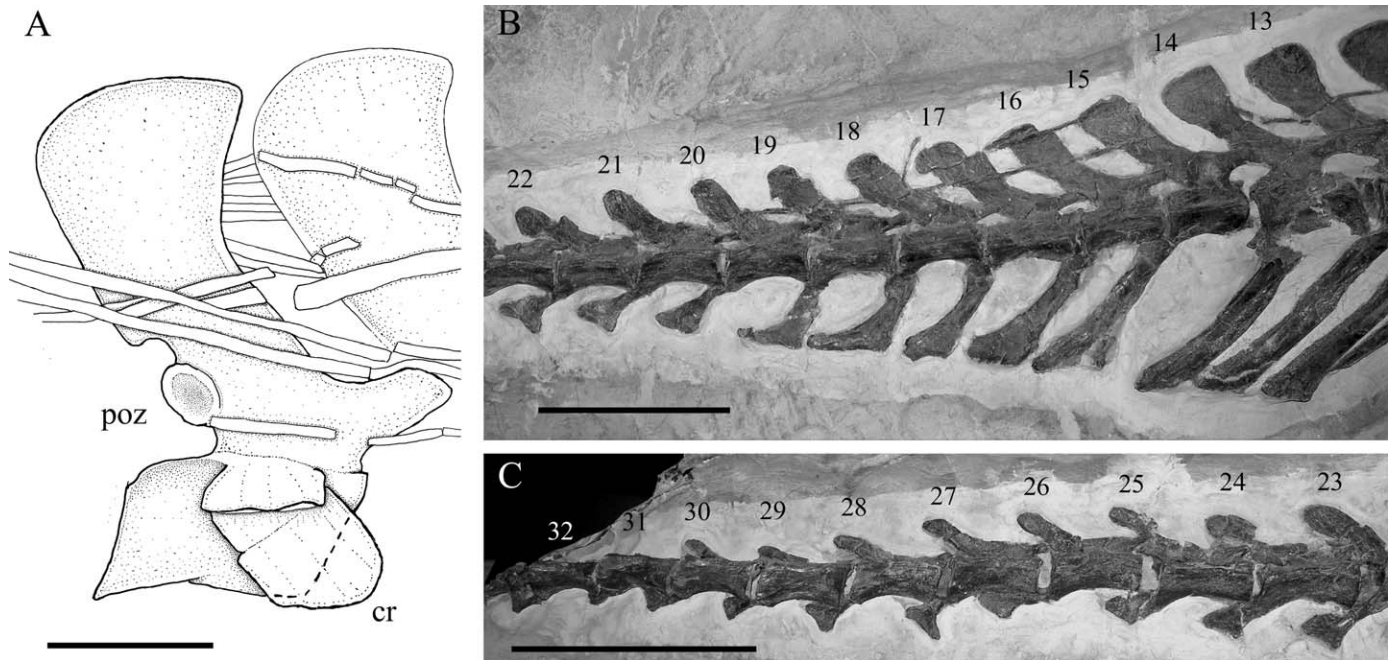
FIGURE 4. Caudal vertebrae of *Tethyshadros insularis*, SC 57021, holotype. Proximal caudal 4 (**A**); middle caudal vertebrae (**B–C**). The progressive number of the elements is reported. **Abbreviations**: **cr**, caudal rib; **poz**, postzygapophysis. Scale bar equals 50 mm.

Dorsal Ribs—There are 13 dorsal ribs per side. They show no appreciable differences with those of *Iguanodon* (see Norman, 1980). The ribs increase in length up to the fifth (∼ 510 mm long), then decrease in length to the 13th.

Sacral Vertebrae—The poor preservation of the sacrum prevents a direct count of the sacral vertebrae. Five vertebrae follow the dorsal vertebra 16 based on the diapophyses, the most caudal occurring in correspondence of the beginning of the postacetabular process of ilium. Comparison with the sacral count in *Gryposaurus incurvimanus* (see Parks, 1920) and the spacing of the diapophyses of sacral vertebrae 1–5, suggest that room exists for three additional sacral vertebrae. Hadrosaurids have 9–12 sacral vertebrae (including dorsosacrals and caudosacrals; Horner et al., 2004), the synsacrum of *Bactrosaurus* has seven vertebrae (Godefroit et al., 1998), as well as that of *Dollodon* where the first synsacral vertebra is nevertheless considered a dorsal (Norman, 1986).

Caudal Vertebrae—The proximal caudal vertebrae are preserved in the holotype and in SC 57247. The caudal segment of the holotype is formed by 33 articulated vertebrae and is about 1650 mm long. I consider the first caudal vertebra as the first one with a fused tongue-shaped rib. There are 13 (possibly 14) proximal caudal vertebrae, followed by 20 (possibly 19) middle caudal vertebrae. The whole distal segment of the tail (at least 10 vertebrae, probably more) remained in situ. Caudal centra are elongate along the whole series. The length:height ratio is 1.48 and 1.22 in caudal vertebrae 4 and 5 respectively. Although those vertebrae are slightly deformed, their centra are undoubtedly longer than high as is the case for all proximal centra, also in SC 57247. This condition is unlike in *Iguanodon* and hadrosauroids where the most proximal centra are higher than long and are often very short (e.g., Parks, 1920; Lull and Wright, 1942; Norman, 1980, 1986, 2002, 2004; Godefroit et al., 1998; Horner et al., 2004; Dalla Vecchia, 2006; pers. obs.). Distally, centra become gradually more elongated, nearly rod-like (Fig. 4B, C). The length:height ratio (measured at mid-centrum) ranges from 1.26 to 3.40 from caudal 11 to 32. The centra of caudal vertebrae 23 to 33 are semi-cylindrical, with a semicircular posterior artic-

ular face, a flat dorsal surface and robust caudal processes for the articulation of the chevrons. The caudal processes for the chevrons start at caudal vertebra 7. Articular facets are present cranially on the centra at least up to caudal vertebra 22. The centra are amphicoelous at least beginning with caudal vertebra 8, and the articular surfaces of the last 15 vertebrae are deeply concave. The caudal ribs are tongue-shaped in caudal vertebrae 1–5, very flattened dorsoventrally, and directed laterally. In caudal vertebrae 6 to 11, they are still flattened but are narrower caudocranially and rapidly reduce in length. Caudal vertebrae 12 and 13 (possibly 14 too) have just small, wing-like, lateral knobs. The postzygapophysis is just a raised, circular facet at the base of the neural spine (Fig. 4A). The nearly vertical zygapophyseal facets of the first caudal vertebrae show that little lateral movement of the tail was possible. The neural spines change in shape along the vertebral series. Those in caudal vertebrae 1 to 6 are caudocranially wide, laterally flat and hatched-shaped (Fig. 4A). The height of the neural spine of caudal vertebra 4 (83 mm) is 2.1 times the centrum height (the height of the neural arch is 2.7 times the centrum height). The neural spines of caudal vertebrae 7 to 16 are fan-shaped in lateral view and are inclined backward (Fig. 4B). The spines of the vertebrae 18 to 30 are caudocranially narrower and are not fan-shaped.

Haemapophyses—Twenty-six haemal arches are preserved articulated to the corresponding facets of the centra. The first haemal arch articulates between caudal vertebra 7 and 8. In contrast, it articulates distal to caudal vertebra 4 or 5 in hadrosaurines and 2 or 3 in lambeosaurines (Horner et al., 2004), between caudal vertebra 2–3 in *Iguanodon* and basal hadrosauroids (Norman, 2004), and between vertebrae 3–4 in *Ouranosaurus* (Taquet, 1976). The position of the first chevron in *Tethyshadros* is more posterior than in all other iguanodontians, thus it is considered an autapomorphic feature.

The chevrons show a marked change in shape along the vertebral series. Chevrons 1–5 have a rod-like shaft that is unexpanded distally. Chevrons 6–26 gradually become shorter and the distal end is expanded and flattened in lateral view. A posterior process is present distally in chevrons 6–11, which reaches its

maximum length in chevrons 12 and 13, before reducing in length in successive chevrons. Chevrons 9-13, which occur between caudal vertebrae 15 and 20, are boot-like. Chevrons with this shape have not reported in other hadrosauroids, where the haemal arches are just laterally compressed rods (e.g., Lull and Wright, 1942; Norman, 1986, 2004; Horner et al., 2004).

Ossified Tendons—Ossified tendons occur epaxially from dorsal vertebra 4 to caudal vertebra 20. In the dorsal segment of the column, most of them cross the series of spines rostroventrally to caudodorsally at a low angle. A few seem to reach the upper part of the spine; most are bundled at its base (Fig. 1). The tendons reach their maximum development in the last dorsal vertebrae and in the sacral segment of the column. Unlike the precaudal segment, ossified tendons cross diagonally the spines, with a cross-lattice pattern, in the caudal vertebrae 1–6 (Figs. 1, 4A). From caudal vertebra 7 to 14, tendons cross the spines at a low angle, mainly rostroventrally to dorsocaudally. The caudal-most tendons are few, thin, and crossing the side of the neural spine mainly posteroventrally to craniodorsally (Fig. 4B).

Appendicular Skeleton

The distance between the acetabulum and the humeral glenoid is 840 mm. The forelimb (humerus + ulna) is 59% the hind limb length (femur + tibia); the tibia is 131% the femur length; and the metatarsal III is 35% the tibial length.

Coracoid—The coracoid is dorsoventrally taller than mediolaterally long (132 and ∼85 mm respectively). In mediocaudal view, the coracoid foramen is close the dorsal edge at the junction between the glenoid and the sutural surface for the scapula; it is somewhat opened dorsally. It opens in a more internal position on the laterorostral surface of the coracoid. The length of the scapular suture in mediocaudal view is slightly greater than that of the glenoid. The glenoid and scapular processes are thick, whereas the lunate portion of the coracoid is thinner, ending ventrally in a hooked sternal process. A slightly thickened 'acromion' ridge forms the dorsal part of the craniomedial margin.

Scapula—The scapula is a strap-like bone 353 mm long, curved and with a blade much expanded distally (Fig. 5A). The ventrocaudal margin is markedly concave. The dorsocranial edge is angled in the proximal third, then is straight and parallel to the ventrocaudal margin and finally flares distally. The blade is extremely thin at the distal expansion and is markedly asymmetric, like that of basal iguanodontians *Dryosaurus* and *Camptosaurus*, and apomorphic among hadrosauroids. The neck is very poorly defined. The thick proximal part of the right scapula of the holotype is damaged in the area corresponding to the sutural surface for the coracoid. A pseudoacromion process pointing laterally is probably absent; there is a small medial flange on the dorsoproximal end of the scapula. This could be another apomorphy of *Tethyshadros*, but the region is poorly preserved and further information is needed to confirm it. The proximal part of the scapula is clearly dorsocranially to ventrocaudally narrow like that of hadrosaurids rather than expanded and with a pseudoacromion process pointing dorsocranially like in *Iguanodon* and some basal hadrosauroids such as *Mantellisaurus*, *Dollodon*, *Ouranosaurus* and *Probactrosaurus*.

Sternal Plates—The paired sternal plates are hatchet-shaped as in *Iguanodon* and hadrosauroids. The caudolateral process ('handle') is narrow and long, over twice longer than the craniomedial plate measured from the distal to the proximal extremities. The caudoventral process of the craniomedial plate is short and projects caudoventrally a distance less than average width of the 'handle.'

Humerus—The humerus in caudal view is slender and slightly sigmoid (Fig. 6A). The deltopectoral crest appears as a gentle outward swelling of the lateral margin, merging into the shaft
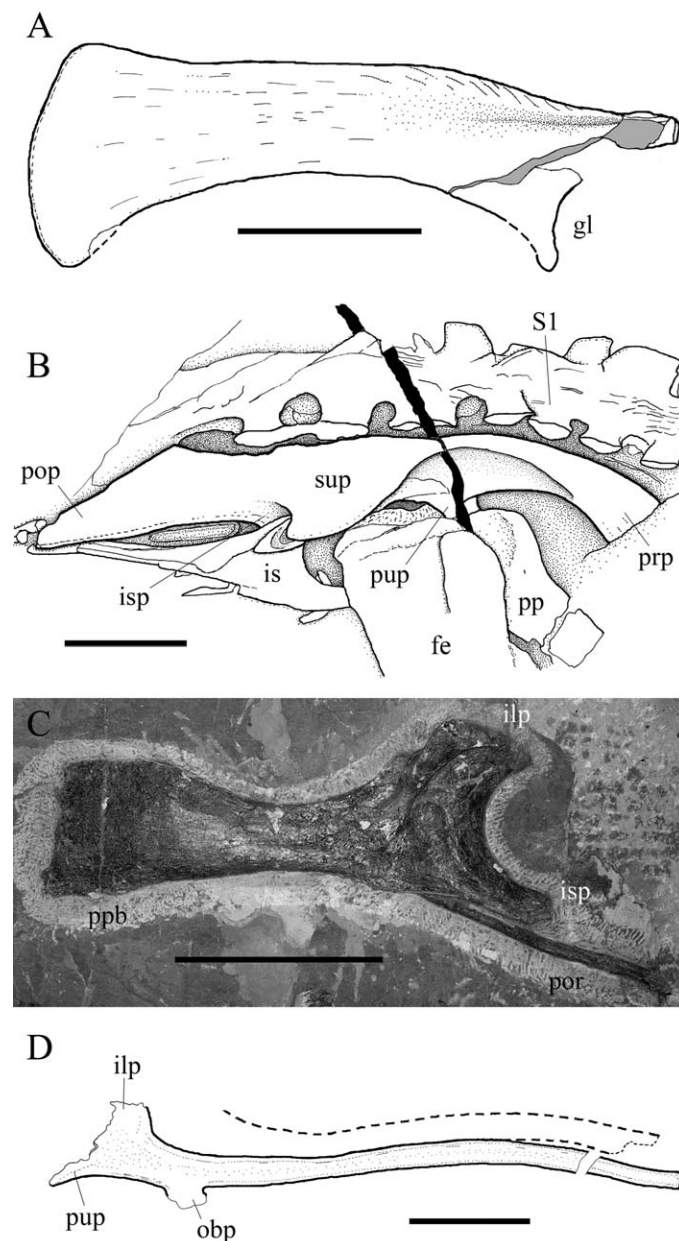
FIGURE 5. Bones of the girdles of *Tethyshadros insularis*. **A**, right scapula of SC 57021, holotype, lateral view; **B**, right ilium of SC 57021, lateral view; **C**, left pubis SC 57023, lateral view; **D**, ischia of SC 57247. **Abbreviations**: **fe**, femur; **gl**, humeral glenoid; **ilp**, iliac process; **is**, ischium; **isp**, ischial process; **obp**, obturator process; **pop**, postacetabular process; **por**, posterior pubic ramus (pubis s. s.); **pp**, prepubic process of pubis; **ppb**, prepubic blade; **prp**, preacetabular process; **pup**, pubic process; **S1**, first sacral vertebra; **sup**, supracetabular process. Shaded areas in outline represent regions where the bone is cross-sectioned or strongly damaged. Scale bar equals 100 mm.

slightly below midshaft. The crest is slightly curved cranially (Fig. 6B), thus it appears larger in the right humerus (Fig. 6C), where it is compressed against the shaft of the left humerus. It is much longer than wide and the point of maximum curvature is just above the midpoint, i.e., it is nearly symmetric without a steep distal margin. The distal condyles are separated caudally by a relatively shallow intercondylar groove. The radial condyle is the largest in caudal view. The left humerus is 3.5% longer
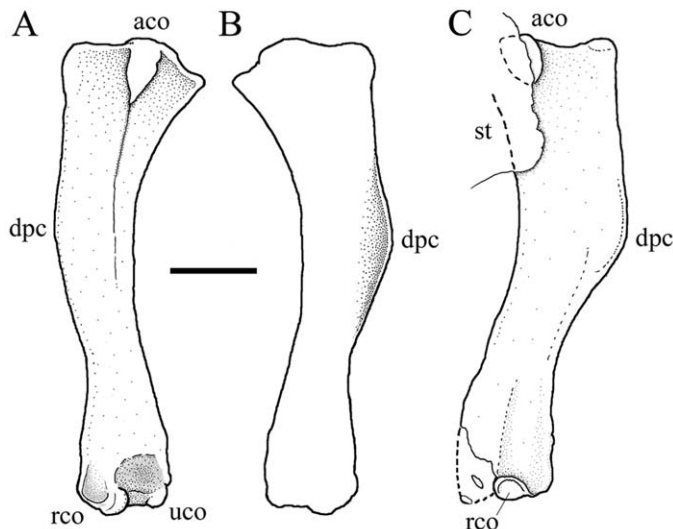
FIGURE 6. Humeri of *Tethyshadros insularis*, SC 57021, holotype. **A**, left, caudal view; **B**, left, cranial view; **C**, right, caudal view. **Abbreviations**: **aco**, articular condyle (caput humeri); **dpc**, deltopectoral crest; **rco**, radial condyle; **st**, sternal plate; **uco**, ulnar condyle. Scale bar equals 50 mm.

than the right; the left humerus is longer than left ulna whereas it is the reverse for the elements of the right side (Table).

Antebrachium—Radius and ulna are slender bones, slightly sigmoid and with moderately expanded proximal and distal extremities. The radius lies cranial to the ulna. The ulna has a modestly developed olecranon process, whose lateral surface is slightly offset and with a rough surface. A robust and arched

flange projects craniolaterally from the proximal part of the bone bordering laterally the wide radial notch.

Carpus—The carpus is reduced to a single, small (10.5 mm the maximum diameter), lozenge-shaped sesamoid-like element. In the right and perfectly articulated forelimb of the holotype, it occurs between the radius and the metacarpal II (Fig. 7B).

Manus—The elements of the left and right hand in both SC 57021 and SC 57022 have different lengths (Table). Metacarpal I is absent. Metacarpals IV to II are elongate, slender, straight and closely appressed to form a single functional unit (Fig. 7B). There is no evidence of metacarpal V in the perfectly articulated right hand, nor in the slightly disarticulated left hand (Fig. 7A, B). Also the articulated mani of SC 57022 lack a metacarpal V (Fig. 7C). Therefore, metacarpal V and the entire digit V are considered apomorphically lost. Metacarpal III is the longest, metacarpal II the shortest (Table). The proximal end of metacarpal III is aligned with those of metacarpals II and IV. The proximal termination of metacarpals IV and III is slightly expanded, and has several neurovascular foramina and a convex articular surface. Metacarpal II is flattened craniocaudally, especially in the proximal third. The distal termination of the metacarpals is flat; this can be appreciated on the left hand where the proximal phalanges are slightly detached (Fig. 7A). The articulation of the phalanges to the respective metacarpals in the right hand (Fig. 7B) precludes the presence of a thick cartilage cap on the distal articular end of the metacarpals.

The phalangeal formula is 0-3-3-2-0. The morphology of the phalanges is complex. Phalanx II–1 is elongate and flattened craniocaudally, with asymmetrically expanded extremities giving it a sigmoid outline in lateral view. Phalanx II–2 is small and wedge-shaped, with the wider side caudal; it fits in a depression of the broad and nearly flat distal articular surface of phalanx II–1. Ungual phalanx II is rough and spongy-looking, lateropalmarily flattened, and expanded hammer-head like. Phalanx III–1 in dorsal view is broad, with a nearly rectangular outline and a
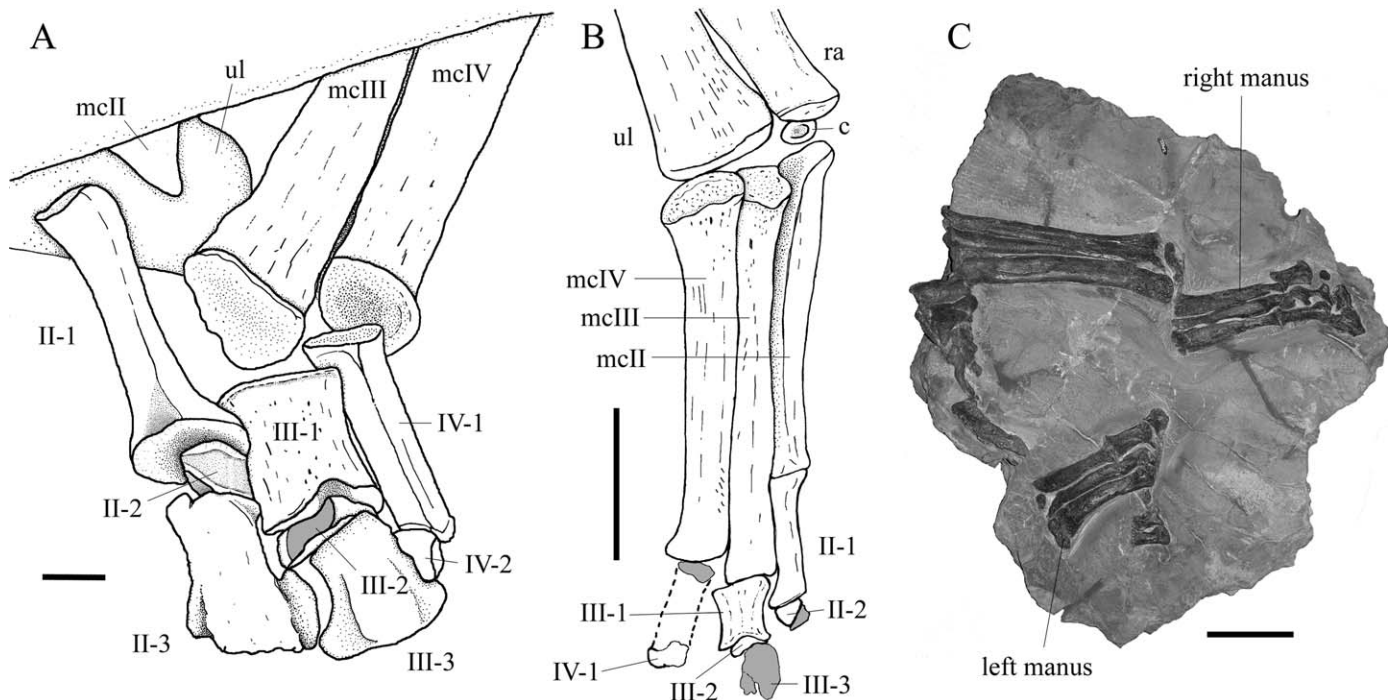
FIGURE 7. Mani of *Tethyshadros insularis*. **A**, Phalangeal portion of the left manus of SC 57021, holotype, lateral view; **B**, right manus of SC 57021, holotype, lateral view; **C**, SC 57022, palmar view. **Abbreviations**: **II–1**, **II–2**, **II–3**, phalanges 1 to 3 of digit III; **III–1**, **III–2**, **III–3**, phalanges 1 to 3 of digit II; **IV–1**, **IV–2**, phalanges 1 and 2 of digit IV; **c**, carpal; **mcII-IV**, metacarpals II-IV; **ra**, radius; **ul**, ulna. Shaded areas in outline represent regions where the bone is sectioned or strongly weathered. Scale bar equals 10 mm (A), 50 mm (B) and 100 mm (C).

TABLE. Measurements (axial lengths, if not specified otherwise) in millimeters of skeletal elements of *Tethyshadros insularis* specimens SC 57021 (holotype) and SC 57022.

Element	SC 57021	SC 57022	Element	SC 57021	SC 57022
Skull	475	—	Femur	420	—
Skull (height)	ca.175	—	Tibia	550	—
Quadrate	ca. 155	—	Metatarsal II	160	—
Lower jaw	390	—	Metatarsal III	193	—
Humerus	287(297)	—	Metatarsal IV	153	—
Ulna	290(280)	+235	P.phalanx II-1	58	—
Radius	280(274)	+280	P.phalanx II-2	14	—
Metacarpal II	105(100)	115(+100)	P.phalanx II-3	25	—
Metacarpal III	128(120)	ca.145(+130)	P.phalanx III-1	52	—
Metacarpal IV	119(116)	125(125)	P.phalanx III-2	10	—
M. phalanx II-1	41(42)	44(53)	P.phalanx III-3	ca. 4	—
M. phalanx II-2	7(8)	ca.10	P.phalanx III-4	28	—
M. phalanx II-3	(27.5)	34(ca.21)	P.phalanx IV-1	48	—
M. phalanx III-1	18(21)	30(ca.30)	P.phalanx IV-2	7	—
M. phalanx III-2	5(6)	ca. 5	P.phalanx IV-3	ca. 4	—
M. phalanx III-3	(19)	18	P.phalanx IV-4	ca. 4	—
M. phalanx IV-1	(32)	44(41)	P.phalanx IV-5	37	—
M. phalanx IV-2	(6.5)	12			—

Measurements of the phalanges are merely indicative because of the difficulty in measuring articulated bones.
Abbreviations: **ca.**, approximately; **M**, manual; **P**, pedal; **+** incomplete element; measurements of left-side elements are in parentheses.

nearly flat lateral surface. The distal termination is bicondylar and phalanx III–2 fits in the groove between the two condyles. In palmar view, phalanx III–1 is sharply convex and Y-shaped because of a robust longitudinal ridge giving the bone a triangular cross section. Phalanx III–2 is wedge-shaped, and very narrow proximodistally. Ungual phalanx III–3 is smaller than that of digit II, lateropalmarily flattened and with a similar morphology. The palmar side has a median longitudinal ridge sided by two elliptical depressions. Phalanx IV–1 is an elongate bone apparently flattened craniocaudally (unless, rotated, in such a case it would be lateropalmarily flattened) and roughly rectangular in this view. The cranial surface is flat, whereas the caudal one is convex. In the right phalanx IV–1 of SC 57022, the distal termination is expanded lateropalmarily and with an arched distal margin, resembling the same phalanx in *G. incurvimanus* (see Parks, 1920:pl.V). A knob occurs close to the distal end of the probable caudal surface. Phalanx IV–2 is still articulated to phalanx IV–1 in the left digit of the holotype; it is very small, and roughly wedge-like in lateral view (Fig. 7A). In SC 57022, it is a small, circular bone close to phalanx IV–1, resembling the phalanx IV–3 of some hadrosaurids (Brown, 1912; Parks, 1920). This suggests that the original phalanx IV–2 of other hadrosauroids was lost. No other phalanx occurs distal to phalanx IV–2, nor are other separated elements visible in either specimen. Therefore, I assume that *Tethyshadros* has apomorphically only two phalanges on digit IV, instead of three as usual in the other hadrosauroids (Norman, 2004; Horner et al., 2004).

Ilium—The ilium is very long and low (Fig. 5B). The dorsoventral height of the central body is about 55–60 mm and the total length is 506 mm. However, the distal end of the preacetabular process is truncated by a fault and an unknown amount lost. The dorsal margin of the iliac blade is relatively straight as in basal hadrosauroids, and not distinctly depressed over the supracetabular process and dorsally bowed over the base of the preacetabular process as in hadrosaurids. The preacetabular process is robust, bowed dorsoventrally, although not to the extent observed in the Lambeosaurinae. Its proximal part is bordered dorsally by a robust ridge that is the cranial continuation of the supracetabular process. This ridge makes the preacetabular process dorsally thick in the lateromedial plane. It tapers to merge with the process where the curvature is maximum and height is minimum. Cranial to the end of the ridge, the preacetabular process slightly flares dorsoventrally and is lateromedially flattened. The supracetabular process is very large, wing-like and

asymmetrical (the apex is offset caudally). It overhangs the whole lateral side of the ilium as in hadrosaurids. The low and long (at least 175 mm) postacetabular process is plate-like, without a brevis shelf, and tapers caudally to nearly a point. The ventral margin is nearly straight and horizontal, whereas the dorsal one is angled, with a long, straight and sloping caudal segment. The triangular outline of the process in lateral view is reminiscent of that observed in some of the most basal hadrosauroids (*Mantellisaurus*, *Dollodon*, *Ouranosaurus* and *Probactrosaurus*; Norman, 2004, 2002; Paul, 2008) and is unlike the process in hadrosaurids (Brett-Surman and Wagner, 2007). The ischial process, distally covered by the iliac process of the right ischium, seems to be very scarcely projecting. Also the shape of the pubic process cannot be fully appreciated, but it was craniocaudally narrow, ventrorostrally directed and probably rather short.

Pubis—The isolated left pubis SC 57023 (Fig. 5C), exposed in lateral view, is smaller than that of the holotype (the length measured from the cranial margin of the iliac process to the distal tip of the prepubis is 210 mm and ∼300 mm, respectively), but similar in shape, resembling that of the lambeosaurine hadrosaurid *Lambeosaurus magnicristatus* (see Evans and Reisz, 2007). The iliac process is very large and robust, whereas the ischial one is more slender. The prepubis in lateral view has a shallowly concave ventral margin and a dorsal edge that is concave corresponding to the neck, then is straight in the distal part of the blade. The neck is narrow and the prepubic blade is expanded dorsoventrally, two times the minimum constriction of the neck. The cranial edge of the blade is straight and perpendicular to its long axis. The posterior pubic ramus (pubis proper) is straight, thin and rod-like; its distal part is not preserved.

Ischium—The ischia are strongly crushed and stretched in the holotype. The shaft of the left ischium is nearly complete in SC 57247, but the proximal part is damaged (Fig. 5D). The ischium of SC 57247 is about 85 cm long. The iliac process is much larger than the pubic process (as observed also in the holotype). The damaged obturator process is blade-like. The shaft in lateral view is elongated, lateromedially flattened and slightly sigmoid, and not tapering distally. The distal end has just a blunt, unexpanded termination; it is not boot-shaped nor has a knob-like structure. This morphology is not reported in other hadrosauroids (Godefroit et al., 1998; Norman, 2004; Weishampel et al., 2004; Prieto-Marquez et al., 2006; Brett-Surman and Wagner, 2007). Ischia are also comparatively longer than in other

hadrosauroids, a lengthening related to the posterior displacement of the haemapophyses.

Femur—The femur is a relatively stout bone, with a straight shaft. The cranial trochanter is flattened by crushing against the greater trochanter. There are no traces of the thin 4th trochanter that, being placed mediocaudally, it could be covered by the shaft and probably was broken by crushing and pieces were possibly lost during preparation. The medial distal condyle is well developed and expanded both cranially and caudally. The lateral distal condyle is also slightly expanded cranially and caudally and sends caudally a long, lateromedially flattened condylid process. Because the femur is only visible in lateral view, nothing can be said about the caudal and cranial intercondylar grooves.

Tibia and Fibula—The tibia differs from that of other hadrosauroids only for being markedly longer than femur (550 mm against 420 mm). It is always shorter than femur in basal hadrosauroids and hadrosaurids (see Lull and Wright, 1942; Norman, 2004) excluding the basal hadrosauroid *Nanyangosaurus* (see Xu et al., 2000) and the lambeosaurine *Olorotitan arharensis* (P. Godefroit, pers. comm). It is a slender and straight bone, with a thin and broad cnemial crest with a rounded profile. The outer, shorter malleolus is wrapped caudally by two flat bones representing caudal projections of the proximal tarsals. The fibula is distally shorter than tibia and much thinner; it twists around the tibial shaft to end on its craniolateral side. Its proximal end is only moderately flared and not boot-shaped.

Tarsus—No evidence of the astragalus can be seen in the damaged caudal view of the inner malleolus of the right tibia. The better preserved outer malleolus is covered cranially by the calcaneum that caps its extremity sending on the caudal surface a small, tongue-like process. Another similar, tongue-like and apparently separated bone caps the distocaudal surface of the malleolus more medially, possibly representing the caudolateral process of the astragalus. Only an isolated tarsal 4 occurs close to the proximal articular surface of the right metatarsal IV; it is small (28 mm the main axis), elliptical and flat in proximal view. Probably the distal tarsals 2 and 3 are absent.

Pes—There is no trace of a metatarsal I. Metatarsals II–IV are relatively elongated, metatarsal III is the longest and metatarsal II is just slightly longer than metatarsal IV (Table). They are interlocked proximally, parallel and closely appressed along most of their shafts and bear distal condyles. The articular surface is oriented distoposteriorly and small dorsodistal processes are developed to avoid a digital hyperextension. The distal portion of metatarsals II and IV is slightly deflected medially and laterally respectively; possibly the distal part of metatarsal IV is offset also plantarily. They show no substantial differences from the metatarsals of the other hadrosauroids. The phalangeal formula is 0-3-4-5-0. The phalangeal portion of the digits is rather short (Table), with digit III slightly more projecting than digit II and IV. The first pedal phalanges of all three digits are robust, longer than wide, with expanded proximal ends and distal bicondylar trochleae, enormously developed in II–1, and much less in IV–1. The other non-ungual phalanges are very short proximodistally. Phalanx IV–2 is disc-like, with two shallow depressions in the proximal facet for the distal condyles of phalanx 1. Two disc-like phalanges IV–3 and IV–4 occurs between phalanx IV–2 and the ungual phalanx, and are much smaller. The width of phalanx III–2 is over four-times its length; phalanx III–3 is disc-like and much shorter. Phalanx II–2 has a subrectangular outline in dorsal view and is possibly wedge-shaped, with the distal articular surface oriented distoplantarily to articulate on the dorsoproximal, wide articular surface of the ungual phalanx. The unguals are short and dorsoplantarily flattened, with a proximal stem and a distal expansion. The spade-shaped ungual of digit IV has a very rough dorsal surface. The ungual phalanx of digit III is similarly rough in aspect, but with a hammer-head

shape, whereas that of digit II has an expanded distal part reduced and misshapen.

PHYLOGENETIC ANALYSIS

A phylogenetic analysis by parsimony was performed using PAUP*4.0b10 for Microsoft Windows (Swofford, 2002) in order to assess the phylogenetic position of *Tethyshadros insularis*. I used the heuristic search option and the ACCTRAN character state optimization. Characters were given equal weight and multistate characters where treated as unordered. The dataset includes three outgroups (*Iguanodon bernissartensis*, *Mantellisaurus atherfieldensis* and *Dollodon bampingi*), 22 ingroup taxa (including basal hadrosauroids and hadrosaurine and lambeosaurine hadrosaurids) and 121 characters. The data matrix (see supplementary data at http://www.vertpaleo.org/publications/JVPContent.cfm) is basically that of Prieto-Marquez et al. (2006), with some deletions, emendations and corrections, and the addition of seven further characters. Characters 24, 81, and 76–79 of Prieto-Marquez et al. (2006) were eliminated and character 11 was replaced by two new characters based on A. Prieto-Marquez's suggestions. Phylogenetically uninformative characters were also eliminated. Some character definitions were modified mainly to adapt them to the state present in *Tethyshadros*. *Telmatosaurus* character states were also modified when what directly observed on the specimens was contrasting with the codings in Prieto-Marquez et al. (2006). I modified the character states for other taxa when the published description and figures of the specimens were in evident contrast with that coded in Prieto-Marquez et al. (2006). In case of doubt, the codings of Prieto-Marquez et al. (2006) are maintained. Unlike Prieto-Marquez et al. (2006), *Iguanodon atherfieldensis* was split into *M. atherfieldensis* and *D. bampingi* according to Paul (2008).

The analysis produced 55 equally parsimonious trees with a length of 370 steps, consistency index = 0.5757, retention index = 0.7819 and rescaled consistency index = 0.4501. The phylogenetic analysis indicates that *Tethyshadros insularis* is outside the Hadrosauridae and close to *Telmatosaurus*, although its actual phylogenetic relationship is not resolved (Fig. 8). It forms a politomy with *Telmatosaurus* and all the more derived hadrosauroids in the Strict Consensus Tree (Fig. 8A). In the 55 equally parsimonious trees, it is either the sister taxon of *Telmatosaurus* (*Tethyshadros* and *Telmatosaurus* forming a clade), or more derived than *Telmatosaurus* and is the sister taxon of all more derived hadrosauroids (*Telmatosaurus* is the sister taxon of *Tethyshadros* + all more derived hadrosauroids), or less derived than *Telmatosaurus* (sister taxon of *Telmatosaurus* + all more derived hadrosauroids). According to the 50% Majority Rule Consensus Tree (Fig. 8B), *Tethyshadros* is more derived than *Telmatosaurus* and is the sister taxon of the Hadrosauridae. The exclusion of the poorly resolved *Pararhabdodon* (which results a basal Lambeosaurinae or the sister taxon of Hadrosauridae in the analysis) drastically reduces the number of equally parsimonious trees from 55 to 4, but this regards only the stability of the Lambeosaurinae and the Hadrosaurinae and has no effect on the position of *Tethyshadros* in the cladogram.

DISCUSSION

Comparison to Other Hadrosauroid Dinosaurs

Tethyshadros insularis has a mixture of derived (e.g., hadrosaurid) and primitive characters found in more basal hadrosauroids, suggesting a mosaic evolution of the features characterizing hadrosaurids, showing that some of them (e.g., those in the locomotory apparatus) were reached before others.

Primitive features of *Tethyshadros* include the overall skull morphology, reminiscent of that of *Iguanodon* (see Norman, 1980), *Mantellisaurus* (see Paul, 2008) and *Dollodon* (see Norman, 1986)

Iguanodon bernissartensis
Mantellisaurus atherfieldensis
Dollodon bampingi
Ouranosaurus nigeriensis
Probactrosaurus gobiensis
Protohadros byrdi
Bactrosaurus johnsoni
Gilmoreosaurus mongoliensis
Tanius sinensis
Telmatosaurus transsylvanicus
Tethyshadros insularis
Pararhabdodon isonensis
Gryposaurus spp.
Edmontosaurus spp.
Brachylophosaurus canadensis
Maiasaura peeblesorum
Prosaurolophus spp.
Saurolophus spp.
Hypacrosaurus altispinus
Hypacrosaurus stebingeri
Amurosaurus riabinini
Lambeosaurus spp.
Corythosaurus casuarius
Parasaurolophus spp.
Olorotitan arharensis

A

B

Iguanodon bernissartensis
Mantellisaurus atherfieldensis
Dollodon bampingi
Ouranosaurus nigeriensis
Probactrosaurus gobiensis
Protohadros byrdi
Bactrosaurus johnsoni
Gilmoreosaurus mongoliensis
Tanius sinensis
Telmatosaurus transsylvanicus
Tethyshadros insularis
Edmontosaurus spp.
Brachylophosaurus canadensis
Maiasaura peeblesorum
Gryposaurus spp.
Prosaurolophus spp.
Saurolophus spp.
Pararhabdodon isonensis
Hypacrosaurus altispinus
Hypacrosaurus stebingeri
Amurosaurus riabinini
Lambeosaurus spp.
Corythosaurus casuarius
Parasaurolophus spp.
Olorotitan arharensis

FIGURE 8.   Phylogenetic hypothesis of relationships of *Tethyshadros* to other hadrosauroids. **A**, Strict Consensus Tree; **B**, 50% Majority Rule Consensus Tree.

in being elongated and having a moderately expanded muzzle, large rostral denticles on premaxilla, a supraorbital bone, and a conspicuous participation of the surangular in the posterior part of the coronoid process. Other non-hadrosaurid characters are a leaf-shaped rostral process of the jugal and the absence of a mandibular diastema. Unlike hadrosaurids and *Telmatosaurus*, the lateral mandibular condyle is not hemispherical and the medial condyle is not much smaller and higher in the quadrate. The dentary teeth are comparatively wider than those of most hadrosaurids (crown height:width ratio is 2.5), with mesial and distal subsidiary ridges, and small marginal denticles usually lacking in hadrosaurid teeth. Probably there were no more than two replacement teeth per tooth family, whereas adult hadrosaurids have three or more. Also maxillary teeth have denticulated margins and sometimes a faint, mesial, subsidiary ridge. The neck is short (11 cervical vertebrae; hadrosaurids have 12 or more) and the sacrum has a relatively low number of vertebrae (probably 8 compared with 9–12 in hadrosaurids). The distal part of the scapular blade resembles that of the iguanodontians *Camptosaurus* and *Dryosaurus*, more basal than *Iguanodon* (see Norman, 2004). The humerus has a primitive aspect, with a deltopectoral crest little projecting from the shaft and not angled. The postacetabular process of the ilium is triangular in lateral view like in some very basal hadrosauroids.

Like hadrosaurids and *Telmatosaurus*, *Tethyshadros* lacks an antorbital fenestra between lacrimal and maxilla (but retains a shallow fossa) and a finger-like jugal process in the maxilla. The quadratojugal notch is a wide embayment (a 'paraquadrate' foramen cannot be present), there is no surangular foramen, dentary teeth form a battery with at least two functioning teeth per family, and there are possibly sclerotic bones. There is a pronounced U-like curvature of the neck and cranial part of the dorsal axial skeleton that is typical of hadrosaurids (Horner et al., 2004). The proximal part of the scapula is more similar to that of hadrosaurids than the expanded form of *Iguanodon* and basal-most hadrosauroids. Although the ilium has a relatively straight dorsal margin like in basal hadrosauroids, it possesses a large, wing-like supracetabular process, a feature often considered synapomorphic of hadrosaurids and absent in *Iguanodon* and basal hadrosauroids (Norman, 2004; Horner et al., 2004; Gilpin et al., 2007). Mani and pedes show the highest grade of modification from the *Iguanodon* primitive condition. The carpus is extremely reduced and the pollex was lost, as well as the entire digit V. Manual digits have slender metacarpals, wedge-like second phalanges in digits II and III, and short, broad and lateropalmarily flattened ungual phalanges. The phalangeal portion of the pedal digits is rather short as in hadrosaurids, phalanges between the first phalanx and the ungual are disc-like, and the ungual phalanges are dorsoplantarily flattened, broad, short and with a rough, irregular morphology.

Basal hadrosauroids and hadrosaurids are relatively common in the upper Campanian–Maastrichtian of Europe, but are represented only by very incomplete remains (Weishampel et al., 2004; Dalla Vecchia, 2006). Only two Late Cretaceous hadrosauroid species have been named in Europe to date: *Telmatosaurus transsylvanicus* from the lower Maastrichtian of Romania (Nopcsa, 1900, 1928; Weishampel et al., 1993) and *Pararhabdodon isonensis* from the Maastrichtian (probably upper Maastrichtian) of Spain (Prieto-Marquez et al., 2006). *Koutalisaurus kohlerorum*, also from the Maastrichtian of Spain (Prieto-Marquez et al., 2006), is possibly a younger synonym of the latter. *Telmatosaurus*, the best known of them, is actually based on an array of scattered, fragmentary bones and several parts of the skeleton are unknown (Dalla Vecchia, 2006). Only the maxillae and a few postcranial bones represent *P. isonensis*, and *K. kohlerorum* is based on a single dentary (Prieto-Marquez et al., 2006).

Besides features listed elsewhere in this paper, *Tethyshadros* differs from *Telmatosaurus* also in having a smaller supratemporal fenestra, a less massive frontal and with slender flanges,
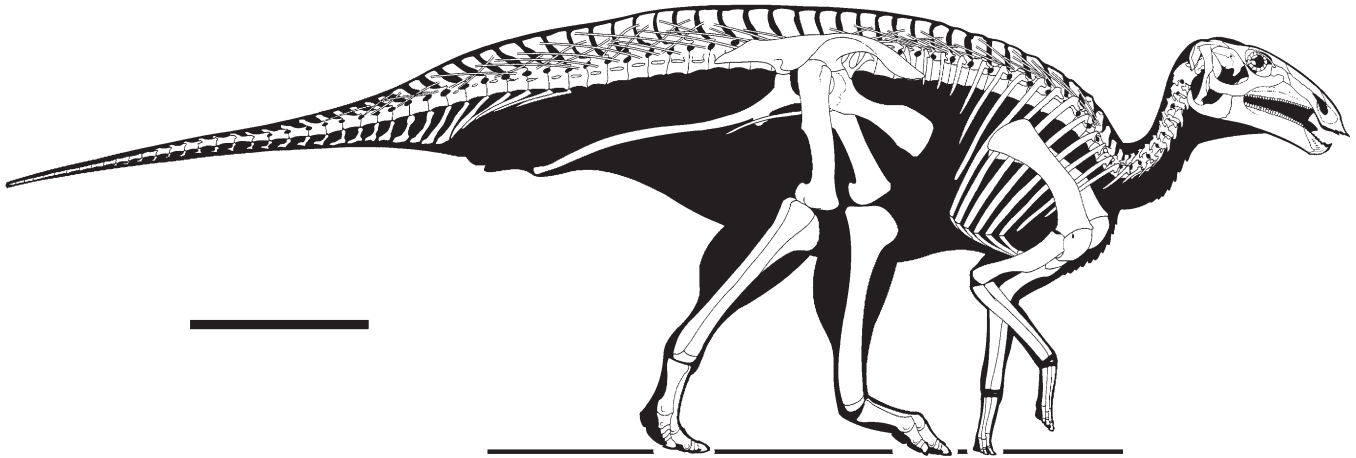
FIGURE 9. Skeletal reconstruction of *Tethyshadros insularis*. Scale bar equals 500 mm.

a bent quadrate, a rostral process of the jugal not triangular nor pointed, a depression in the maxilla in the position of the antorbital fenestra of more basal hadrosauroids, closely packed dentary teeth with up to three separated mesial accessory ridges and distal accessory ridges as well, smaller marginal denticles and a straight upper part of the crown, maxillary teeth sometimes bearing a thin mesial subsidiary ridge and with a more rounded apex of the crown, cervical vertebrae with postzygapophyses less tall and not dorsolaterally splayed, neural spines in proximal caudal vertebrae with a different morphology (Nopcsa, 1928: pl.5, fig. 6), and probably the femur was not bowed.

Functional Morphology

The features suggesting subunguligrady in the hadrosaurid *Corythosaurus* and *Saurolophus* (Moreno et al., 2006) are found also in *Tethyshadros*: tridactyly, digit shortening, hoof-like unguals, phalanges much wider than long, lack of collateral ligament fossae, relatively flattened articular surfaces (at least in the elements distal to the first phalangeal row).

Tethyshadros shows skeletal features occurring in cursorial amniotes (Coombs, 1978): tibia longer than femur, lateral digits lost and metapodials long, slender and interlocked, acting as a single element, reduction in the mass of the foot (by losing or shortening of the phalanges, and narrowing of the metapodials) and the subunguligrade stance. In the plot of hind limb proportions of bipedal and quadrupedal non-avian dinosaurs with various degrees of cursorial limb structure by Coombs (1978:fig. 9), *Tethyshadros* has a relatively low metatarsal III:tibia ratio (0.35; similar to that of the hadrosaurid *Corythosaurus casuarius*) and a very high tibia:femur ratio (1.31; similar to that of the small bipedal ornithischian *Heterodontosaurus tucki*). It falls at the margin of the dinosaur distribution and close to the plots of small bipedal ornithischians.

The peculiar shape of the proximal part of the tail (i.e., the length of the portion without chevrons, the elongation of the centra, the shape of the ribs and chevrons; Fig. 9) might be related to a great development and elongation of the caudofemoral musculature, the main femur retractor (Gatesy, 1990; Dilkes, 2000), also suggesting a cursorial attitude.

The carpus is reduced to a single small carpal, the manual digit I is lost as well as digit V and a phalanx in digit IV. The metacarpals are slender, elongate and closely appressed, with flat distal articular surfaces as are those of most phalanges, thus no flection was possible at the metatarsal–phalangeal joint and in most intra-phalangeal joints. The penultimate phalanges of manual digits II and III are wedge-shaped and the unguals II and III are hoof-like. Proximal phalanges appear as a prolongation of metacarpals and the whole hand looks like a pillar. Grasping ability was evidently very limited and the manus acted as a single unit with a small terminal surface. Apparently, it could be used only in quadrupedal locomotion, although its gracility and reduced terminal surface, as well as the probable orientation, suggest a prevalent role of support during resting, and balance during moving bipedally. It is possibly an adaptation to a peculiar life style (i.e., moving on rough grounds, like those common in karst landscapes).

Paleobiogeography

Tethyshadros lived at the northern end of a wide carbonate platform, the Adriatic–Dinaric Carbonate Platform (ADCP), a paleogeographic unit of the Adria Microplate. During Aptian to Eocene times, ADCP was a Bahamas-like bank in the Tethys Ocean between the Afro-Arabian Continent and the North European landmass (Eberli et al., 1993; Camoin et al., 1993; Philip, Floquet et al., 2000) and part of the European Archipelago (Weishampel et al., 1993) (Fig. 10). It was repeatedly emergent locally, but siliciclastic sediments deposited in continental environments are absent. A latest Cretaceous tectonic event affected its northern termination. A peripheral, migrating foreland bulge, due to the advancing flexural foreland profile, was caused by the vertical loading of the Adria microplate by the Alpine orogenetic wedge (Otoničar, 2007) and is the cause for the emergence that allowed the presence of the hadrosauroid dinosaurs.

The Adriatic–Dinaric Island had a maximum estimated surface approximately 100,000 km^2 (based on Camoin et al., 1993), comparable to that of Cuba today. All individuals represented in the sample are much smaller than average North American adult hadrosaurids (Weishampel et al., 1993) and lack evidence of osteological immaturity suggestive of a juvenile condition. This small size might plausibly be due to insular dwarfism (e.g., Azzaroli, 1982; Lomolino, 1985), a phenomenon already observed in other insular dinosaurs (Jianu and Weishampel, 1999; Dalla Vecchia et al., 2001; Sander et al., 2006). The axial and appendicular skeleton is rather conservative in continental hadrosaurids (Horner et al., 2004) and more basal hadrosauroids (Norman, 2004; Paul, 2008), but presents several apomorphies in *Tethyshadros*. The presence of unusual features might also be related to insularism (Azzaroli, 1982).
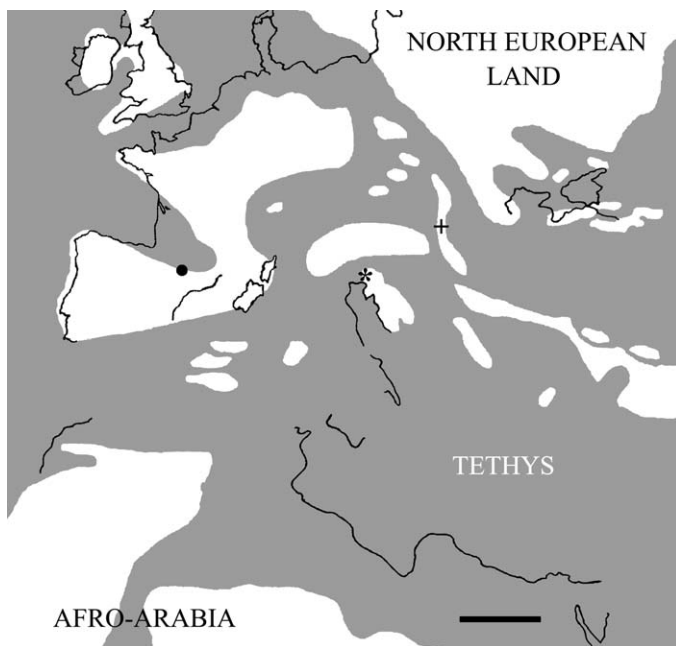
FIGURE 10. The European Archipelago of the western Tethys during Maastrichtian times, based on Camoin et al. (1993), with location of the sites that yielded hadrosauroid taxa. **Symbols**: **asterisk**, the Villaggio del Pescatore site; **cross**, the site of *Telmatosaurus*; **black dot**, the site of *Pararhabdodon* and *Koutalisaurus*. **Colors**: white, land; gray, sea. Scale bar equals 500 km.

The primitiveness of *Telmatosaurus* and other hadrosauroids of the European Archipelago compared to coeval or even older hadrosaurids of western North America has been explained as due to localized, conservative evolution in isolation since the middle Cretaceous (Weishampel et al., 1993) (vicariance model). However, the ADCP was isolated in the Tethys at least since the Aptian (Dercourt et al., 1993) and was drowned during the latest Cenomanian-Turonian marine high stand (Gušić and Jelaška, 1993). Before Aptian it might have been connected to Afro-Arabia (Bosellini, 2002) where as yet, no post–Aptian hadrosauroid fossils have been reported (Weishampel et al., 2004). Similarly, dinosaurs living on the ADCP before latest Cretaceous times were mainly sauropods and theropods (Dalla Vecchia, 1998; Dalla Vecchia and Tarlao, 2000; Dalla Vecchia et al., 2001, 2002). Instead, only hadrosauroids are identified from Villaggio del Pescatore and hadrosauroid and theropod teeth are recorded in the close and roughly coeval site of Kozina (Slovenia) (Debeljak et al., 1999). A late Santonian dinosaur assemblage in Hungary and the early Campanian assemblages of France and Austria, lack hadrosauroids (Weishampel et al., 2004). Instead, they occur in the upper Campanian–Maastrichtian of Spain, France, The Netherlands, Belgium, Germany, Slovenia, Italy, Romania and Ukraine (Weishampel et al., 2004; Dalla Vecchia, 2006). They spread during the Maastrichtian, whereas they were much rarer in the late Campanian. In the European Archipelago, the dominant Santonian–early Maastrichtian ornithopods were the endemic rhabdodontids (Weishampel et al., 2002, 2004).

The successive sister taxa of *Tethyshadros* and *Telmatosaurus* are the Asiatic *Bactrosaurus*, *Gilmoreosaurus* and *Tanius* from the Campanian–Maastrichtian (Weishampel et al., 2004; Van Itterbeeck et al., 2005), and the most basal Hadrosaurinae know to date comes from the Maastrichtian of northern China (Godefroit et al., 2008). North American basal hadrosauroids are only Barremian–Turonian in age (Weishampel et al., 2004; McDonald et al., 2006; Gilpin et al., 2007), whereas the well-known Campanian–

Maastrichtian hadrosauroids of North America are all hadrosaurids (Horner et al., 2004; Weishampel et al., 2004). Unlike North America, non-hadrosaurid hadrosauroids might be common in Eurasia during the latest Cretaceous. All of this supports an Asiatic origin of the European taxa. Hadrosauroids may have colonized the European Archipelago from Asia (dispersal model) where non-hadrosaurid hadrosauroids were still living during Campanian–early Maastrichtian times. Microplate collisions along the northern margins of Tethys occurred during the first stages of Alpine orogeny (e.g., Neugebauer et al., 2001), caused the formation of the Transylvanian Island where *Telmatosaurus* lived, the emergence of the Adriatic–Dinaric Island of *Tethyshadros*, and connections in the eastern parts of the European Archipelago (e.g., Therrien, 2005; Otoničar, 2007; De Min et al., 2007) (Fig. 10). In addition, tectonic crustal uplift and volcanism along the geodynamically active northern margin of Tethys might also create emergent lands and a migration route with southern Asia. The hadrosauroids most probably reached the eastern part of the European Archipelago by dispersal through insular hopping along the south-western margin of Asia. This dispersal event, probably the first of a series of dispersal events, might have happened during the late Campanian.

LITERATURE CITED

Arbulla, D., F. Cotza, F. Cucchi, F. M. Dalla Vecchia, A. De Giusto, O. Flora, D. Masetti, A. Palci, P. Pittau, N. Pugliese, B. Stenni, A. Tarlao, G. Tunis, and L. Zini. 2006. Escursione nel Carso Triestino, in Slovenia e Croazia. 8 giugno. Stop 1. La successione Santoniano–Campaniana del Villaggio del Pescatore (Carso Triestino) nel quale sono stati rinvenuti i resti di dinosauro; pp. 20–27 in R. Melis, R. Romano, and G. Fonda (eds.), Guida alle escursioni/excursions guide, Società Paleontologica Italiana – Giornate di Paleontologia 2006. EUT Edizioni Università di Trieste, Trieste.

Azzaroli, A. 1982. Insularity and its effects on terrestrial vertebrates: evolutionary and biogeographic aspects; pp. 193–213; in E. Montanaro Gallitelli (ed.), Palaeontology, Essential of Historical Geology. STEM Mucchi, Modena, Italy.

Bosellini, A. 2002. Dinosaurs "re-write" the geodynamics of the eastern Mediterranean and the palaeogeography of the Apulia Platform. Earth–Sciences Review 59:211–234.

Brett-Surman, M. K., and J. R. Wagner. 2006. Discussion on character analysis of the appendicular anatomy in Campanian and Maastrichtian North American hadrosaurids – variation and ontogeny; pp. 135–169 in K. Carpenter, (ed.), Horns and beaks–Ceratopsian and ornithopod dinosaurs. Indiana University Press, Bloomington and Indianapolis, Indiana.

Brown, B. 1912. The osteology of the manus in the Family Tracho-dontidae. Bulletin of the American Museum of Natural History 31:105–108.

Camoin, G., Y. Bellion, J. Dercourt, R. Guiraud, J. Lucas, A. Poisson, L. E. Ricou, and B. Vrielynck. 1993. Late Maastrichtian palaeoen-vironments (69.5 to 65 Ma); in J. Dercourt, L. E. Ricou, and B. Vrielynck (eds.), Atlas Tethys, Palaeoenvironmental Maps. BEICIP–FRANLAB, Rueil–Malmaison, France.

Carpenter, K. 1994. Baby *Dryosaurus* from the Upper Jurassic Morrison Formation of Dinosaur National Monument; pp. 288–297 in K. Carpenter, K. F. Hirsch, and J. R. Horner (eds.), Dinosaurs eggs and babies. Cambridge University Press, Cambridge, U.K.

Coombs, W. P., Jr. 1978. Theoretical aspects of cursorial adaptations in dinosaurs. Quarterly Review of Biology 53:393–418.

Dalla Vecchia, F. M. 1998. Remains of Sauropoda (Reptilia, Saurischia) in the Lower Cretaceous (Upper Hauterivian/Lower Barremian) limestones of SW Istria (Croatia). Geologia Croatica 51:105–134.

Dalla Vecchia, F. M. 2006. *Telmatosaurus* and the other hadrosaurids of the Cretaceous European Archipelago. An overview. Natura Nas-costa 32:1–55.

Dalla Vecchia, F. M. 2008. I dinosauri del Villaggio del Pescatore (Trieste): qualche aggiornamento. Atti del Museo Civico di Storia Naturale di Trieste – numero speciale: 111–129.

Dalla Vecchia, F. M., and A. Tarlao. 2000. New dinosaur track sites in the Albian (Early Cretaceous) of the Istrian peninsula (Croatia). Part II – Paleontology. Memorie di Scienze Geologiche 52:227–293.

Dalla Vecchia, F. M., A. Tarlao, G. Tunis, and S. Venturini. 2001. Dino-saur track sites in the upper Cenomanian (Late Cretaceous) of the Istrian peninsula (Croatia). Bollettino della Società Paleontologica Italiana 40:25–54.

Dalla Vecchia, F. M., I. Vlahovic, L. Posocco, A. Tarlao, and M. Tentor. 2002. Late Barremian and Late Albian (Early Cretaceous) dinosaur track sites in the Main Brioni/Brijun Island (SW Istria, Croatia). Natura Nascosta 25:1–36.

Debeljak, I., A. Košir, and B. Otoničar. 1999. A preliminary note on dinosaurs and non-dinosaurian reptiles from the Upper Cretaceous carbonate platform succession at Kozina (SW Slovenia). Razprave IV. Razreda Sazu 40:3–25.

Delfino, M., and E. Buffetaut. 2006. A preliminary description of the crocodilian remains from the Late Cretaceous of Villaggio del Pes-catore (Northeastern Italy); p. 33 in Abstracts–Giornate di Paleon-tologia 2006. Società Paleontologica Italiana–Trieste.

De Min, A., Rosset, A., Tunis, G., Kocmann, C., Tosone, A. and Lenaz, D. 2007. Igneous rock clasts from the Maastrichtian Bovec flysch (Slovenia): petrology and geodynamic aspects. Geologia Carpathica 58:169–179.

Dercourt, J., L. E. Ricou, and B. Vrielynck (eds.) 1993. Atlas Tethys, Palaeoenvironmental Maps. BEICIP–FRANLAB, Rueil–Malmai-son, France.

Dilkes, D. W. 2000. Appendicular myology of the hadrosaurian dinosaur *Maiasaura peeblesorum* from the Late Cretaceous (Campanian) of Montana. Transactions of the Royal Society of Edinburgh: Earth Sciences 90:87–125.

Eberli, G. P., D. Bernoulli, D. Sanders, and A. Vecsei. 1993. From aggradation to progradation. The Maiella Platform (Abruzzi, Italy). AAPG Memoires 56:213–232.

Evans, D. C., and R. R. Reisz. 2007. Anatomy and relationships of *Lambeosaurus magnicristatus*, a crested hadrosaurid dinosaur (Ornithischia) from the Dinosaur Park Formation. Alberta. Journal of Vertebrate Paleontology 27:373–393.

Gatesy, S. M. 1990. Caudofemoral musculature and the evolution of theropod locomotion. Paleobiology 16:170–186.

Gilmore, C. W. 1933. On the dinosaurian fauna of the Iren Dabasu Forma-tion. Bulletin of the American Museum of Natural History 67:23–78.

Gilpin, D., T. DiCroce, and K. Carpenter. 2007. A possible new basal hadrosaur from the Lower Cretaceous Cedar Mountain Formation of Eastern Utah; pp. 79–89; in K. Carpenter, (ed.) Horns and beaks–Ceratopsian and ornithopod dinosaurs. Indiana University Press, Bloomington and Indianapolis, Indiana.

Godefroit, P., Z.-M. Dong, P. Bultynck, H. Li, and L. Feng 1998. Sino–Belgian Cooperation Program "Cretaceous Dinosaurs and Mam-mals from Inner Mongolia". 1. New *Bactrosaurus* (Dinosauria: Hadrosauroidea) material from Iren Dabasu (Inner Mongolia, P. R. China). Bulletin de l'Institut Royal des Sciences Naturelles de Belgique–Sciences de la Terre 68(supp.):3–70.

Godefroit, P., S. Hay, T. You, and P. Lauters. 2008. New hadrosaurid dinosaurs from the uppermost Cretaceous of northeastern China. Acta Palaeontologica Polonica 53:47–74.

Gušić, I., and V. Jelaška. 1993. Upper Cenomanian-lower Turonian sea-level rise and its consequences on the Adriatic-Dinaric Carbonate Platform. Geologische Rundschaft 82:676–686.

Horner, J. R., and P. J. Currie. 1994. Embryonic and neonatal morphol-ogy and ontogeny of a new species of *Hypacrosaurus* (Ornithischia, Lambeosauridae) from Montana and Alberta; pp. 312–336 in K. Carpenter, K. F. Hirsch, and J. R. Horner (eds.), Dinosaurs eggs and babies. Cambridge University Press, Cambridge, U.K.

Horner, J. R., D. B. Weishampel, and C. A. Forster. 2004. Hadrosauridae; pp. 438–463 in D. B. Weishampel, P. Dodson, and H. Osmólska (eds.), The Dinosauria 2nd edn. University of California Press, Berkeley, California.

Jianu, C.-M., and D. B. Weishampel. 1999. The smallest of the largest. A new look at possible dwarfing in sauropod dinosaurs. Geologie en Mijnbouw 78:335–343.

Jurkovšek, B., M. Toman, B. Ogorelec, L. Sribar, K. Drobne, M. Poljak, and L. Sribar. 1996. Geological map of the southern part of the Trieste–Komen Plateau. Cretaceous and Paleogene carbonate rocks. Scale 1:50.000. Institut za Geologijo, geotehniko in geofiziko, Ljubljana, Slovenia, 143 pp. and map.

Van Itterbeeck, J., D. J. Horne, P. Bultynck, and N. Vandenberghe. 2005. Stratigraphy and palaeoenvironment of the dinosaur-bearing Upper Cretaceous Iren Dabasu Formation, Inner Mongolia, People's Republic of China. Cretaceous Research 26:699–725.

Lambe, L. M. 1920. The hadrosaur *Edmontosaurus* from the Upper Creta-ceous of Alberta. Geological Survey of Canada, Memoir 120:1–79.

Lomolino, M. V. 1985. Body size of mammals on islands; the island rule reexamined. The American Naturalist 125:310–316.

Lull, R. S., and N. E. Wright. 1942. Hadrosaurian dinosaurs of North America. Geological Society of America Special Papers 40:1–242.

Marsh, O. C. 1882. Classification of the Dinosauria. American Journal of Science (Third Series) 23:81–96.

Martin, J. E. 2007. New material of the Late Cretaceous globidontan *Acynodon iberoccitanus* (Crocodylia) from southern France. Journal of Vertebrate Paleontology 27:362–372.

Maryańska, T., and H. Osmólska. 1979. Aspects of hadrosaurian cranial anatomy. Lethaia 12:265–273.

McDonald, A. T., D. G. Wolfe, and J. I. Kirkland. 2006. On a hadrosar-omorph (Dinosauria: Ornithopoda) from the Moreno Hill Forma-tion (Cretaceous, Turonian) of New Mexico. New Mexico Museum of Natural History and Science Bulletin 35:277.

Moreno, K., M. T. Carrano, and R. Snyder. 2006. Morphological changes in pedal phalanges through ornithopod dinosaur evolution: a biome-chanical approach. Journal of Morphology 268:50–63.

Neugebauer, J., B. Greiner, and E. Appel. 2001. Kinematics of the Alpine–West Carpathian orogen and paleogeographic implications. Journal of the Geological Society of London 158:97–110.

Nopcsa, F. 1900. Dinosaurierreste aus Siebenbürgen (Schädel von *Lim-nosaurus transsylvanicus* nov. gen. et spec.). Denkschriften der köni-glichen Akademie der Wissenschaften, Wien 68:555–591.

Nopcsa, F. 1928. Dinosaurierreste aus Siebenbürgen. IV. Die wirbelsäule von *Rhabdodon* und *Orthomerus*. Palaeontologia Hungarica 1 (1921–1923):273–304.

Norman, D. B. 1980. On the ornithischian dinosaur *Iguanodon bernissar-tensis* from the Lower Cretaceous of Bernissart (Belgium). Institut Royal des Sciences Naturelles de Belgique–Mémoire 178:1–100.

Norman, D. B. 1986. On the anatomy of *Iguanodon atherfieldensis* (Ornithischia: Ornithopoda). Bulletin de l'Institut Royal des Sciences Naturelles de Belgique, Sciences de la Terre 56:281–372.

Norman, D. B. 2002. On Asian ornithopods (Dinosauria: Ornithischia). 4. *Probactrosaurus* Rozhdestevensky, 1966. Zoological Journal of the Linnean Society, London 136:113–144.

Norman, D. B. 2004. Basal Iguanodontia; pp. 413–437; in D. B. Weishampel, P. Dodson, and H. Osmólska (eds.), The Dinosauria 2nd edn. Univer-sity of California Press, Berkeley, California.

Otoničar, B. 2007. Upper Cretaceous to Paleogene forebulge unconformity associated with foreland basin evolution (Kras, Matarsko Podolje and Istria; SW Slovenia and NW Croatia). Acta Carsologica 36:101–120.

Parks, W. A. 1920. The osteology of the trachodont dinosaur *Kritosaurus incurvimanus*. University of Toronto Geological Studies 11:1–74.

Paul, G. 2008. A revised taxonomy of the iguanodont dinosaur genera and species. Cretaceous Research 29:192–216.

Philip, J., and M. Floquet. et al. 2000. Map 16. Late Maastrichtian (69.5 to 65 Ma); in J. Dercourt and M. Gaetani et al. (eds.), Atlas Peri-Tethys, Palaeogeographical Maps. CCGM/CGMW, Paris, France.

Prieto-Marquez, A. 2007. Postcranial osteology of the hadrosaurid dinosaur *Brachylophosaurus canadensis* from the Late Cretaceous of Montana; pp. 91–115; in K. Carpenter, (ed.), Horns and beaks– Ceratopsian and ornithopod dinosaurs. Indiana University Press, Bloomington and Indianapolis, Indiana.

Prieto-Marquez, A., R. Gaete, G. Rivas, À. Galobart, and M. Boada. 2006. Hadrosaurid dinosaurs from the Late Cretaceous of Spain: *Pararhabdodon isonensis* revisited and *Koutalisaurus kohlerorum*, gen et sp. nov. Journal of Vertebrate Paleontology 26:929–943.

Sander, M. P., O. Mateus, T. Laven, and N. Knötschke. 2006. Bone histology indicates insular dwarfism in a new Late Jurassic sauropods dinosaur. Nature 441:739–741.

Sereno, P. 1986. Phylogeny of the bird-hipped dinosaurs (Order Ornithischia). National Geographic Research 2:234–256.

Sereno, P. 1998. A rationale for phylogenetic definitions, with application to higher-level taxonomy of Dinosauria. Neue Jahrbuch für Geologie und Paläontologie, Abhandlungen 210:41–83.

Steuber, T., T. Korbar, V. Jelaška, and I. Gušić. 2005. Strontium-isotope stratigraphy of Upper Cretaceous platform carbonates of the island of Brač (Adriatic Sea, Croatia): implications for global correlation of platform evolution and biostratigraphy. Cretaceous Research 26: 741–756.

Swofford, D. L. 2002. PAUP 4.Ob10. Sinauer Associates, Sunderland, Massachusetts.

Taquet, Ph. 1976. Géologie et paléontologie du gisement de Gadoufaoua (Aptien du Niger). Cahiers de Paléontologie. Editions du Centre National de la Recherque Scientifique, Paris, France, 191 pp.

Therrien, F. 2005. Palaeoenvironment of the latest Cretaceous (Maastrichtian) dinosaurs of Romania: insights from fluvial deposits and paleosols of the Transylvanian and Haṭeg basins. Palaeogeography, Palaeoclimatology, Palaeoecology 218:15–56.

Venturini, S., M. Tentor, and G. Tumis. 2008. Episodi continentali edulcicoli ed eventi biostratigrafici nella sezione campaniano-maastrichtiana di Cotici (M. te San Michele, Gorizia). Natura Nascosta 36:6–23.

Weishampel, D. B., D. B. Norman, and D. Grigorescu. 1993. *Telmatosaurus transsylvanicus* from the Late Cretaceous of Romania: the most basal hadrosaurid dinosaur. Palaeontology 36:361–385.

Weishampel, D. B., C.-M. Jianu, Z. Csiki, and D.B. Norman. 2003. Osteology and phylogeny of *Zalmoxes* (n.g.), an unusual Euornithopod dinosaur from the latest Cretaceous. Journal of Systematic Palaeontology 1:65–123.

Weishampel, D. B., P. M. Barrett, R. A. Coria, J. Le Loeuff, X. Xing, Z. Xijin, A. Sahni, E. M. P. Gomani, and C. R. Noto. 2004. Dinosaur distribution; pp. 517–606 in D. B. Weishampel, P. Dodson, and H. Osmólska (eds.), The Dinosauria 2nd edn. University of California Press, Berkeley, California.

Wiman, C. 1929. Die Kreide-Dinosaurier aus Shantung. Palaeontologia Sinica (ser. C.) 6(1):1–67.

Xu, X., X.-J. Zhao, J.-C. Lü, W.-B. Huang, Z.-Y. Li, and Z.-M. Dong. 2000. A new iguanodontian from Sangping Formation of Nexiang, Henan and its stratigraphical implication. Vertebrata PalAsiatica 38:176–191. [Chinese 176–186; English 186–191].

You, H., Z. Luo, N. H. Shubin, L. M. Witmer, Z. Tang, and F. Tang. 2003. The earliest-known duck-billed dinosaur from deposits of late Early Cretaceous age in northwest China and hadrosaur evolution. Cretaceous Research 24:347–355.